



**Passive Acoustic Monitoring of Cetacean Activity Patterns and
Movements in Minas Passage: Pre-Turbine Baseline Conditions
(2011-2012)**

Final Report

Research Project to funders OERA and FORCE

Research Project duration (June 1 2011 – May 31 2013)

Date of submission: 31 July 2013

Grant Recipients:

Dr. Dominic Tollit, SMRU Limited, 3069 6th Avenue West, Vancouver, BC, Canada
V6K 1X4

Dr. Anna Redden, ACER, Acadia University, Wolfville, NS, Canada, B4P 2R1

| | |
|--------------------------------|---|
| Project Name: | Passive Acoustic Monitoring of Cetacean Activity Patterns and Movements in Minas Passage: Pre-Turbine Baseline Conditions (2011-2012) |
| Reference: | SMRU Ltd code: NA0713Acadia |
| Prepared for: | Fundy Ocean Research Center for Energy (FORCE) and the Offshore Energy Research Association of Nova Scotia (OERANS) |
| Collaborative Partners: | SMRU Ltd. and ACER, Acadia University |

| | | |
|---------------------|--|-----------|
| Drafted by: | Jason Wood, Dominic Tollit, Anna Redden, Peter Porskamp, Jeremy Broome, Lauren Fogarty, Cormac Booth and Richard Karsten | |
| Checked by: | Dominic Tollit | 19/7/2013 |
| Approved by: | | |
| Date: | | |

TABLE OF CONTENTS

| | |
|---|-----|
| TABLE OF CONTENTS..... | ii |
| LIST OF FIGURES..... | iv |
| LIST OF TABLES..... | vi |
| ABSTRACT..... | vii |
| 1.0 INTRODUCTION..... | 1 |
| 1.1 Scope of the Study | 1 |
| 1.2 Passive Acoustic Monitoring of Cetaceans | 3 |
| 2.0 STUDY OBJECTIVES..... | 4 |
| 3.0 SITE DESCRIPTION AND METHODOLOGY..... | 5 |
| 3.1 Site Description | 5 |
| 3.2 Monitoring Sites | 9 |
| 3.3 C-POD Description and Specifications..... | 10 |
| 3.4 C-POD Deployment and Retrieval Success..... | 10 |
| 3.5 C-POD Data Recovery and Processing..... | 12 |
| 3.6 Study Plan Variance..... | 14 |
| 3.7 Data Quality..... | 14 |
| 3.8 Statistical analyses and covariates..... | 16 |
| 3.8.1 Candidate Covariates | 17 |
| 3.8.2 Investigating Singularities and Collinearities | 18 |
| 3.8.3 Model Selection | 19 |
| 3.9 Data Interpretation and Visualization..... | 19 |
| 3.10 Comparing the Performance of Hydrophone Technologies | 20 |
| 3.10.1 icListenHF Description and Specifications | 20 |
| 3.10.2 Range Detection Tests | 21 |
| 3.10.3 Mooring Designs for Co-located Hydrophones | 21 |
| 3.10.4 Hydrophone Deployment and Retrieval..... | 22 |
| 4.0 RESULTS..... | 24 |
| 4.1 Overall Summary of C-POD Detections..... | 24 |
| 4.2 GAM/GEE Model | 25 |
| 4.2.1 Julian Day | 28 |

| | | |
|-------|--|----|
| 4.2.2 | Tidal Height | 29 |
| 4.2.3 | Location..... | 29 |
| 4.2.4 | Day Night Index..... | 30 |
| 4.2.5 | % Time Lost | 30 |
| 4.2.6 | Click Max | 31 |
| 4.3 | Data Interpretation and Visualization: Fine-scale Spatial and Temporal Patterns..... | 31 |
| 4.3.1 | Seasonal Patterns..... | 31 |
| 4.3.2 | Tidal Cycle and Diurnal Patterns Inside FORCE..... | 33 |
| 4.3.3 | Tidal Cycle and Diurnal Patterns Outside FORCE..... | 36 |
| 4.4 | icListenHF vs C-POD Porpoise Detections | 39 |
| 4.4.1 | Comparison of Lost Recording Time | 39 |
| 4.4.2 | Hydrophone DPMs during Ebb and Flood Periods in Aug 2012 | 45 |
| 4.4.3 | Comparison of Overall Detections..... | 48 |
| 5.0 | DISCUSSION..... | 48 |
| 5.1 | Porpoise Activity Trends in Minas Passage | 49 |
| 5.2 | Hydrophone Technology Comparisons | 51 |
| 5.3 | Conclusions and Recommendations | 53 |
| 5.3.1 | Temporal and Spatial Coverage | 53 |
| 5.3.2 | Deployment Methodology..... | 53 |
| 5.3.3 | Alternative Monitoring Tools..... | 53 |
| | ACKNOWLEDGEMENTS..... | 54 |
| | REFERENCES..... | 55 |

LIST OF FIGURES

| | |
|---|----|
| Figure 1. Map of the Maritimes showing the Bay of Fundy and location of the FORCE Crown Lease Area in the Minas Passage, Upper Bay of Fundy, near Parrsboro, Nova Scotia..... | 1 |
| Figure 2. Mean water depths (m) in Minas Passage (top) and the C-POD deployment region (bottom)..... | 7 |
| Figure 3. Predicted flow speeds (m/s) and velocities in the C-POD deployment region during a typical flood tide (top) and a typical ebb tide (bottom) | 8 |
| Figure 4. Multibeam bathymetric map of the FORCE test area, Minas Passage, Bay of Fundy, showing gravel waves, troughs, and various bedforms. | 9 |
| Figure 5. Rigging units for deployment of C-PODs. Mooring chain weights can be seen on the stern of the vessel. Photo courtesy of Colin Buhariwalla. | 11 |
| Figure 6. Data retrieved from C-PODs deployed in Minas Passage by location. Top Panel is 2011 data. Bottom Panel is 2012 data. Date format is dd/mm/yy. | 13 |
| Figure 7. Percent time lost at four locations (W1, E1, E2, S2) during the month of May 2011. Clearly evident are the neap/spring as well as flood/ebb tidal cycles. | 15 |
| Figure 8. Cumulative probability plot of percent time lost for August 2011 across 5 locations. It is clear that E2 and S1 suffer most from sediment noise. | 15 |
| Figure 9. Images of a C-POD (top) and an icListenHF hydrophone (bottom). See Table 4 for specifications. | 20 |
| Figure 10. Specialized SUB buoy mooring designs for the icListenHF hydrophone (left) and the C-POD deployments (right). Mooring components shown are not to scale..... | 22 |
| Figure 11. Locations of C-POD and icListenHF hydrophones deployed on August 1st 2012 within the FORCE test site (1 km x 1.6 km)..... | 23 |
| Figure 12. Example of diagnostically increasing Inter Click Interval of Weak Unknown Transient Signals. | 25 |
| Figure 13. GAM plots of significant covariates and their relationship to porpoise DP10M. Analyses include all data from 2011 and 2012. | 27 |
| Figure 14. DPM per day in Minas Passage. Top trace is the average DPM per day (averaged across locations being monitored). Middle and bottom traces are DPM per day at the two FORCE locations (W1 and E1) in 2011 and 2012, respectively. | 28 |
| Figure 15. Porpoise detections across locations in 2011. Top trace: proportion of C-POD locations with detections during each 10 minute recording period. Bottom trace: number of locations monitored during 2011. | 32 |
| Figure 16. DPMp10M at location W1 highlighting trends across and within month variability. Top trace is spring 2011, middle trace is summer 2011 and the bottom trace is fall 2011. Vertical dashed lines indicate the start of a new day (i.e. midnight). | 33 |

Figure 17. Tidal height (m) across one month periods in the spring, summer and fall. A tidal height of zero is the mean tidal height. Vertical dashed lines indicate the start of a new day (i.e. midnight)..... 34

Figure 18. One week of data from W1 during the spring of 2011. Top trace: Tidal Height (m); Second trace: % Time Lost; Third trace: Tidal Velocity (m/s); Last trace: DPMp10M..... 35

Figure 19. One week of data from W1 during the summer of 2011. Top trace: Tidal Height (m); Second trace: % Time Lost; Third trace: Tidal Velocity (m/s); Last trace: DPMp10M..... 35

Figure 20. One week of data from W1 during the fall of 2011. Top trace: Tidal Height (m); Second trace: % Time Lost; Third trace: Tidal Velocity (m/s); Last trace: DPMp10M..... 36

Figure 21. One week of data from N1 during the spring of 2011. Top trace: Tidal Height (m); Second trace: % Time Lost; Third trace: Tidal Velocity (m/s); Last trace: DPMp10M..... 37

Figure 22. One week of data from N1 during the summer of 2011. Top trace: Tidal Height (m); Second trace: % Time Lost; Third trace: Tidal Velocity (m/s); Last trace: DPMp10M..... 37

Figure 23. One week of data from S2 during the spring of 2011. Top trace: Tidal Height (m); Second trace: % Time Lost; Third trace: Tidal Velocity (m/s); Last trace: DPMp10M..... 38

Figure 24. One week of data from S2 during the summer of 2011. Top trace: Tidal Height (m); Second trace: % Time Lost; Third trace: Tidal Velocity (m/s); Last trace: DPMp10M..... 38

Figure 25. LUCY screenshot showing multiple porpoise click trains within a single minute on August 2nd 2012. 40

Figure 26. Ebb and Flood tide series of LUCY screenshots (one-minute frames) during a spring tidal cycle on August 3rd 2012..... 41

Figure 27. Ebb and Flood tide series of LUCY screenshots (one-minute frames) during a neap tidal cycle on August 11th 2012..... 42

Figure 28. Tidal range and percent lost recording time per day in August 2012 for C-PODs 638, 639, 1520 and icListenHF..... 43

Figure 29. DPM per day, tidal range and percent lost recording time for the icListenHF during the month of August 2012.. 44

Figure 30. Percent lost recording time versus tidal range for a) C-POD 638, b) C-POD 1520, c) C-POD 639, and d) icListenHF. Y-axis scale varies among plots. 45

Figure 31. DPMs/day for both ebb and flood periods for C-POD 638, C-POD 639 and the icListenHF hydrophone during August 2012..... 46

Figure 32. icListenHF detections per minute during August 12th (neap tide) and August 22nd (spring tide)..... 47

Figure 33. One minute LUCY screenshots with a high number of click detection events. Left, both the icListenHF and C-POD recorded a DPM. 48

LIST OF TABLES

| | |
|--|----|
| Table 1. Approximate locations of C-PODs deployed in Minas Passage for this study. Depths are at Mean Water Level..... | 12 |
| Table 2. List of deployments and retrievals by location. | 12 |
| Table 3. List of covariates that were considered in the statistical models and reasons why they were excluded from the final model. | 19 |
| Table 4. Specifications for the icListenHF and C-POD hydrophones used in this study. | 21 |
| Table 5. Duration of recording times for all deployed hydrophones. All hydrophones were deployed on August 1st 2012, at Sites W1 and E1. | 23 |
| Table 6. Descriptive statistics for all porpoise data collected in Minas Passage 2011-12. The same metrics are presented in Table 8 through Table 14 to describe porpoise detection results for individual covariates, for ease of comparison. % of 10MP with DPM is the percentage of 10 minute periods with at least one porpoise detection..... | 24 |
| Table 7. Concordance correlation coefficients (CC) for the significant DP10M covariates retained in the statistical model. Based on these results we were able to rank the importance of each of the covariate..... | 26 |
| Table 8. Descriptive statistics for 30 Julian Days corresponding to the spring and fall peaks and summer trough in Figure 13. % of 10MP with DPM is the percentage of 10 minute periods with at least one porpoise detection..... | 28 |
| Table 9. Descriptive statistics for four Tidal Velocity classes. % of 10MP with DPM is the percentage of 10 minute periods with at least one porpoise detection..... | 29 |
| Table 10. Descriptive statistics for five tidal height classes. A tidal height of zero is the mean tidal height in Minas Passage. % of 10MP with DPM is the percentage of 10 minute periods with at least one porpoise detection..... | 29 |
| Table 11. Descriptive statistics for the seven locations used in this study. % of 10MP with DPM is the percentage of 10 minute periods with at least one porpoise detection. Sites in the FORCE lease area are in bold. Depths are provided in brackets after each location. | 30 |
| Table 12. Descriptive statistics for four Day Night Index classes. % of 10MP with DPM is the percentage of 10 minute periods with at least one porpoise detection..... | 30 |
| Table 13. Descriptive statistics for four % Time Lost classes. % of 10MP with DPM is the percentage of 10 minute periods with at least one porpoise detection..... | 31 |
| Table 14. Descriptive statistics for the two Click Max settings used in this study. % of 10MP with DPM is the percentage of 10 minute periods with at least one porpoise detection. | 31 |
| Table 15. Comparison of percent DPMs recorded by both C-PODs and the icListenHF hydrophone..... | 48 |

ABSTRACT

Currently, there is sparse information available on the near-field effects of tidal in-stream energy conversion (TISEC) devices on marine mammals. There is also little data on the temporal presence and activity of marine mammals in the upper Bay of Fundy (Tollit et al., 2011). Overall, harbour porpoise (*Phocoena phocoena*) are listed by COSEWIC as a species of special concern and represent the most commonly occurring species of cetacean in Minas Passage/Basin, seen year-round in small pods, while white-sided dolphins (*Lagenorhynchus obliquidens*) are believed to visit periodically in the summer. While the risk of direct collision or turbine strike remains a potential concern for marine mammals (Wilson, Batty, Daunt, & Carter, 2007), behavioral or activity level modifications or loss of foraging habitat due to anthropogenic noise disturbance (notably noise during TISEC turbine operation, but also during any foundation construction) and indirectly due to changes in prey populations (such as reef effects due to TISEC turbine presence) are considered two significant data-gaps that need biological assessment before any defensible build-out occurs (Ryan, 2010). The collection of baseline data prior to further TISEC deployments is considered vital in any subsequent post-deployment assessment of changes in cetacean activity levels or spatial use.

Prior to this Research Project, FORCE funded SMRU Ltd (University of St Andrews) and Acadia University to undertake a three month pilot baseline study (10 August 2010 – 23 November 2010) during which three autonomous Passive Acoustic Monitoring (PAM) devices, specifically C-POD hydrophones (autonomous cetacean echolocation click detectors manufactured by Chelonia Ltd), were deployed and recovered in the FORCE demonstration area using custom-made bottom moorings fitted with acoustic releases (Tollit et al., 2011).

This Final Report describes work undertaken in 2011 and 2012, during which seven C-PODs were deployed to expand the spatial and temporal coverage of the pilot baseline study. C-PODs were deployed in a gradient design (Ellis & Schneider, 1997), believed most appropriate to study impacts like noise disturbance and indirect prey effects. During both years of study, 2 devices were located within the demonstration area and 5 outside the area (dependent on recovery of C-PODs), ensuring coverage of shallower waters north and deeper waters south, where prey availability may concentrate cetacean foraging. Battery operated CPODs required multiple (3) deployments per year to cover the time period May to November.

The main objectives of the Research Project were to determine the baseline activity patterns and behavior of key cetaceans (porpoises and dolphins) in the Minas Passage during spring, summer and fall, and to assess how these vary temporally (with respect to time of day, weeks, months and across years), spatially (within and outside the FORCE demonstration area) and

with current patterns (tidal cycles and current velocity). A secondary goal was also to assess (if possible) how these activity patterns vary subsequent to the deployment of TISEC devices or cable-laying operations. This secondary goal could not be achieved as there were no TISEC deployments during the study period. Instead, we conducted a pilot study to assess the performance of another hydrophone technology that was co-deployed with C-PODs in the FORCE test area.

In summary, cetacean baseline data was collected for all three seasons (May – January), but a variety of technical difficulties prevented complete coverage for some units outside of the demonstration area. In spite of this, a total of 1,342 days of data were collected (1,932,410 minutes). Data collected in 2011 and 2012 indicate a daily (98% of days had detections) but typically low level presence of harbour porpoise in Minas Passage (median DPM/day = 22 or 1.5% of each day). No other odontocete cetacean species (i.e., dolphins) was detected during either year of the study.

Porpoise presence was highest during the month of May and lowest during the months of July and August coinciding with the seasonal movement of the summer harbour porpoise population into the Bay of Fundy. A final peak in porpoise presence occurred in late October. While it appears that porpoise activity decreases during winter, winter monitoring would need to be conducted to verify this. The tidal variables of velocity and height had a large impact on porpoise presence in Minas Passage. Porpoise presence peaked at flood tidal velocities from 0.5 to 2.5 m/s and tidal heights of 1.5 to 3.5 m above mean tidal height. At higher flood velocities, porpoise detections decreased. On ebb tides, porpoise presence decreased with increasing tidal velocity. Tidal height had a similar pattern with porpoise detections decreasing as tidal height became more negative. The location of C-POD units did have an effect on porpoise detections. The most plausible explanation for this is the depth at which the C-POD was deployed. The deeper the C-POD unit, the higher the number of porpoise detections. The C-PODs within the FORCE area had relatively high porpoise detections (depth ranges from 52-56 m) while those units in deeper water to the south outside of the FORCE area (84 m) had higher predicted detections. The shallowest unit to the north of the FORCE site (27 m) had the lowest porpoise detections.

Diel (day-night) effects were also evident in the data. Porpoise detections were highest in the early morning hours, just after midnight, while they were at their lowest during early afternoon, just after midday. Sediment noise caused by large current velocities within Minas Passage interfered with our ability to detect porpoise by causing memory saturation of the C-POD units. This impact varied by location with the majority of locations impacted most during spring flood tides (i.e., the fastest tidal velocities). However, two locations outside the FORCE lease area

were heavily impacted on both ebb and flood tides and were thus avoided in year two of this study. In spite of the impact of sediment noise on porpoise detections, we were able to control for sediment noise by including it as a covariate in our statistical modelling and therefore still make predictions at high tidal velocities.

A pilot project to compare the porpoise detection performance of C-PODs with a digital hydrophone and recorder, the iListenHF, was conducted over a one month period in August 2012. This study showed that flow-induced noise, which varies with tidal height and current speed, limits Harbour porpoise detection by both hydrophone types, especially during spring tide cycles. Click train detections per minute in August were greatest on the ebb tide at night during a neap tide. Further concurrent deployments using a combination of C-PODs and digital hydrophones are recommended for comparative and complementary purposes and for greater spatial coverage, especially during peak activity periods (spring and fall). Range testing of hydrophones under different flow scenarios would assist the interpretation of the datasets collected.

Minas Passage is a very challenging location in which to monitor biological and physical processes of importance to testing TISEC devices. In spite of these challenges this two year study on marine mammal presence has succeeded in measuring baseline levels of marine mammal usage of Minas Passage which will be crucial for monitoring potential impacts from TISEC devices after they are installed at FORCE.

1.0 INTRODUCTION

1.1 Scope of the Study

Tidal energy is a largely untapped renewable energy source. Worldwide, only a small number of in-stream tidal turbines have been deployed. The Fundy Ocean Research Center for Energy (FORCE) is a Canadian non-profit institute that owns and operates a facility in the Bay of Fundy, Nova Scotia (Figure 1), where grid connected tidal in-stream energy conversion (TISEC) turbines can be tested and demonstrated. It will enable developers, regulators and scientists to study the performance and interaction of tidal energy turbines with the environment. Presently, there are four berths planned for testing TISEC devices. Baseline information is required to investigate potential marine animal – TISEC interactions.

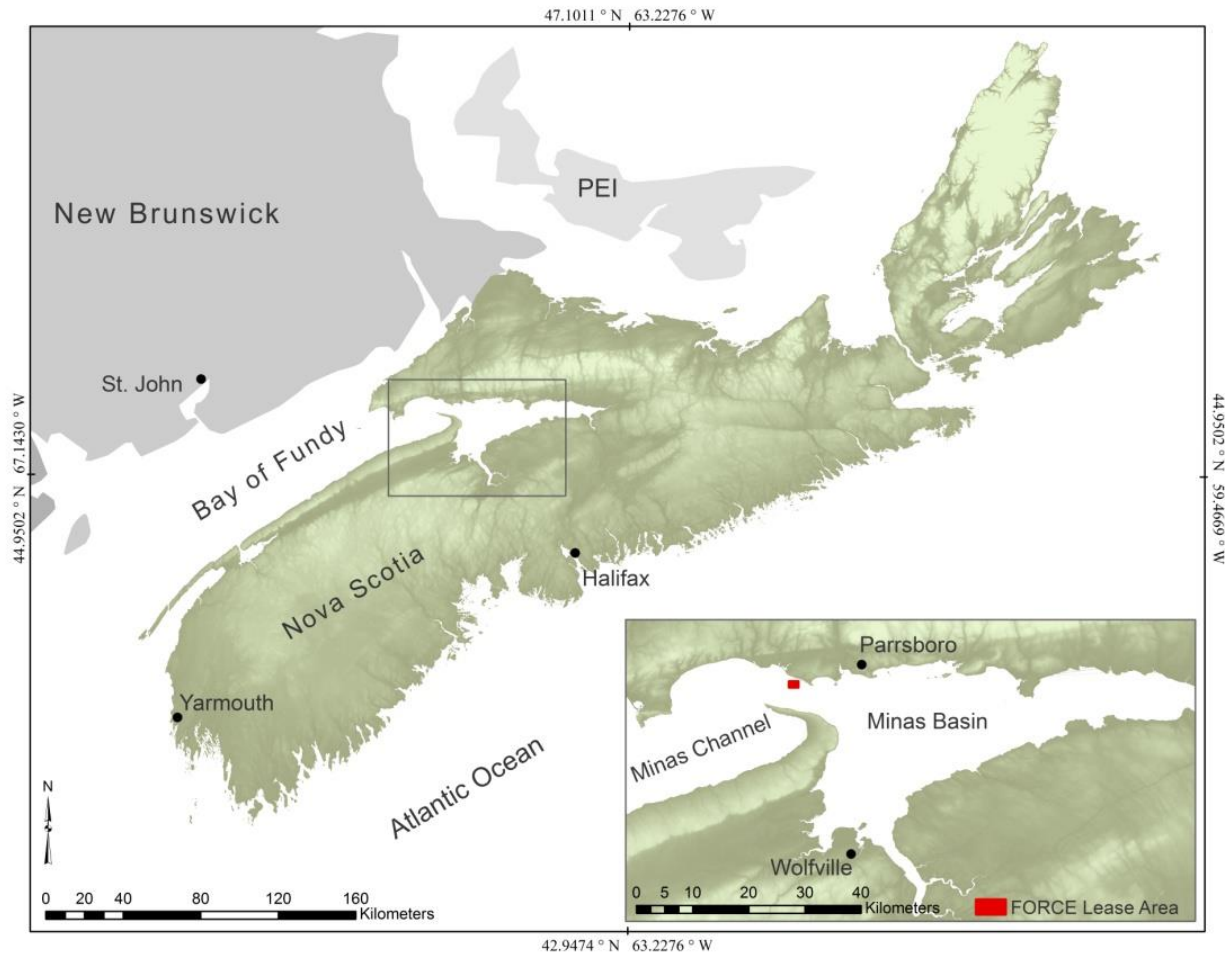


Figure 1. Map of the Maritimes showing the Bay of Fundy and location of the FORCE Crown Lease Area in the Minas Passage, Upper Bay of Fundy, near Parrsboro, Nova Scotia.

Currently, there is sparse information available on the near-field effects of TISEC devices on marine mammals (see database and knowledge management site at http://mhk.pnnl.gov/wiki/index.php/Tethys_Knowledge_Base). A wide range of marine mammals are found in the highly productive outer Bay of Fundy areas, but there is little data on the temporal presence and activity of marine mammals in the upper Bay of Fundy (OEER, 2008). Overall, harbour porpoise (*Phocoena phocoena*) are listed by COSEWIC as a species of special concern and represent the most commonly occurring species of cetacean in Minas Passage/Basin, seen year-round in small pods, while white-sided dolphins (*Lagenorhynchus acutus*) are believed to visit periodically in the summer (Gaskin et al. 1985; OEER 2008). Harbour seals (*Phoca vitulina*) and long-finned pilot whales (*Globicephala melas*) are also reported as common in the upper Bay of Fundy (OEER, 2008).

While the risk of direct collision or turbine strike remains a potential concern for marine mammals (Wilson et al., 2007), behavioral or activity level modifications or loss of foraging habitat due to anthropogenic noise disturbance (notably noise during TISEC turbine operation, but also during any foundation construction) and indirectly due to changes in prey populations (such as reef effects due to TISEC turbine presence) are considered two significant data-gaps that need assessment before any defensible build-out should occur (Ryan, 2010). The collection of baseline data prior to further TISEC deployments is considered vital in any subsequent post-deployment assessment of changes in cetacean activity levels or spatial use.

During 2008-2010, EnviroSphere Consultants Limited undertook two dedicated boat surveys a year (July and August or October) in the vicinity (and waters ~10-15km east and west) of the FORCE demonstration area. No marine mammals were observed in 2008, but 19 harbour porpoise were seen in 2009 (plus also harbour seal, white-sided dolphin, and an unidentified whale) and only five harbour porpoise in the 2010 surveys (EnviroSphere, 2009a; 2010a; 2011a). On each of 7 days in 2010 (May through November), shore-based marine mammal surveys (6 hr) were also completed in a position specifically overlooking the demonstration area (EnviroSphere, 2011a). Small groups (typically 1-3, mode=1, max=7) of harbour porpoise were seen in the study area on five of these days, with one grey seal also observed on one occasion. Across the 84 30min scans undertaken, harbour porpoise were observed in the actual turbine site zone (the area seaward of Black Rock towards the Minas Channel and Cape Split) in 7 (8%) scan periods in total (May 1 (1), June 12 (1), November 13 (4) and November 22 (1)). There did not appear to be an association of the movements with time of day although most individuals were observed from mid- to late in the observation period (typically mid- to late afternoon or early evening) and reported as 'nearly always swimming in the direction of the outgoing tide' (EnviroSphere, 2011a).

1.2 Passive Acoustic Monitoring of Cetaceans

Passive acoustic monitoring (PAM) has become increasingly useful in studies of cetacean habitat use and behaviour, in particular when conditions are unsuitable for land-based observations or boat-based sighting surveys. Conventional sighting surveys for marine mammals are short in duration, expensive and sighting efficiency can be severely affected by weather conditions; it rapidly decreases in rough seas, and is curtailed by factors such as fog, rain and of course darkness. For example, Palka (1996) showed that sighting rates of harbour porpoises dropped sharply in sea states above Beaufort 2. Alternatively, most whales and dolphins are generally highly vocally active and their vocalisations can be detected using underwater microphones (hydrophones); importantly, these PAM systems can operate 24 hours a day, 365 days a year, providing a power source is maintained. Furthermore, sounds produced by different animals frequently exhibit characteristics that, in many cases, allow an identification of their species. For example, the lowest frequency sounds are blue whale moans, which are less than 10Hz and up to 25 seconds in duration. Some of the highest frequency vocalisations are the short narrow band echolocation clicks produced by porpoises which are typically around 0.1 milliseconds and between 100 and 150 kHz in frequency (Au et al., 1999).

Harbour Porpoises are small, shy and unobtrusive (Money and Trites 1998; Olesiuk et al., 2002), making them especially hard to study visually at the ranges required for most study sites. For continuous long-term data collection on porpoises and dolphins, passive acoustic monitoring (PAM) systems are considered effective and recommended (Philpott et al., 2007; Akamatsu et al., 2007; Koschinski, Dierderchs, and Amundin 2008; Todd et al., 2009).

Prior to this Research Project, FORCE funded SMRU Ltd (University of St Andrews) and Acadia University to undertake a three month pilot baseline study (10 August 2010 – 23 November 2010) during which three autonomous Passive Acoustic Monitoring (PAM) devices, specifically C-POD hydrophones (autonomous cetacean echolocation click detectors manufactured by Chelonia Ltd), were deployed and recovered in the FORCE demonstration area using custom-made bottom moorings fitted with acoustic releases (Tollit et al., 2011).

C-PODs are considered a cost-effective autonomous passive acoustic monitoring (PAM) technology and PODs are already in use across Europe and North America for on-going marine renewable impact assessments and site characterization studies (e.g. Cox et al., 2001; Culik et al., 2001; Carlström 2005; Carstensen, Henriksen, and Teilmann 2006; Koschinski et al., 2003; Philpott et al., 2007; Booth et al., 2011; Tollit et al., 2011). C-PODs incorporate a hydrophone, battery pack, memory and a hardware data-logger which detects and logs cetacean echolocation clicks. C-PODs can log data 24 hours a day and are therefore useful at providing continuous data on cetacean activity over extended periods. C-PODs are relatively small, but

are robust and deployed on bottom moorings for single periods of typically 3-4 months (duration dependent on battery life and memory usage), after which they need to be recovered and the data downloaded, with subsequent redeployments being possible. C-POD hydrophones are focused on detecting click trains of porpoise, as well as other species of echolocating delphinids (for example white-sided dolphins). Species can be identified using the dominant frequency of the clicks and the spread of frequencies in the cluster of multipath replicates that are logged. Clicks can also provide basic information on behaviour, such as feeding, using the interval between clicks, which shortens as animals focus in on an object of interest, creating so called 'feeding buzzes'. C-PODs have been shown to detect porpoise-like clicks within a radius of up to ~250m, with effective detection within a ~150-200m radius (Brundiers et al., 2012). It is noted that while useful in determining relative changes in frequency of occurrence or behaviour between sites or through time, they cannot alone provide a count of the number of animals recorded or be used for estimating absolute abundance (Macleod et al., 2010; Kyhn et al., 2012).

Data collected during a pilot study in 2010 (Aug-Nov) indicate porpoise detections on most days (93%), but for short periods averaging ~5 minutes. This represents a daily usage level of 0.3-0.4% of the day (Tollit et al., 2011). No other odontocete cetacean species (i.e., dolphins) was detected during 2010. Porpoise detections were highest (by a factor of more than two) during the night time (23:00 – 1:00) and lowest during the day time (7:00 – 18:00).

This Final Report describes work undertaken in late spring through late fall 2011 and 2012, during which up to 7 C-PODs were deployed at a time. Multiple deployments were required for battery replacements to cover the core time periods from May to November each year.

2.0 STUDY OBJECTIVES

This collaborative two year OERA and FORCE funded Research Project between SMRU Ltd (University of St Andrews) and Acadia University collected information on key cetacean species (marine mammals) using bottom-moored passive acoustic monitoring (PAM) units (C-PODs) deployed in and around the FORCE demonstration area to answer the following research questions:

1. What are the baseline activity patterns and behavior of key cetaceans (porpoises and dolphins) in and near the Force test area in the Minas Passage during spring, summer and fall?
2. How do these activity patterns and behavior vary temporally, with respect to time of day, week, month and across years?

3. How do these activity patterns and behavior relate to tidal cycles, current velocity and temperature?
4. How do these activity patterns and behaviour vary spatially, with respect to PAM units located within and outside the FORCE demonstration area?
5. How do these activity patterns vary subsequent to the deployment of TISEC devices? This objective could not be fulfilled due to a delay in the installation of turbines during the study period.

Although not originally proposed, we deployed a newly developed technology (icListen HF hydrophone, Ocean Sonics Inc.) within the FORCE lease area for the purpose of comparing its porpoise detection performance with that of co-located C-PODS.

3.0 SITE DESCRIPTION AND METHODOLOGY

3.1 Site Description

The Minas Passage is located in the Bay of Fundy, Nova Scotia, Canada and connects the Minas Channel to the Minas Basin (Figure 1). It is a narrow channel, 5-6 km wide and 13 km long, with an average depth of 53 m, and about 150 m at its deepest point (Figure 2). Mean water depths in and around the FORCE lease area range from approximately 25 to 85 meters (Figure 2).

The tide in the Minas Passage is dominated by the M2 tide producing a semi-diurnal tide (high and low tides twice daily), with a period of 12.4 hours. The maximum tidal range in Minas Passage can exceed 13 m; in Minas Basin it can reach as high as 17 m (Karsten et al., 2008). The extreme tidal amplitude in the region is caused by resonance; the depth and geometry of the Bay of Fundy/Gulf of Maine are such that the tidal wave takes slightly longer than $\frac{1}{4}$ period of the M2 tide to transit from the Atlantic Ocean to the tip of Minas Basin (Karsten et al., 2008). During spring tides, current speeds in Minas Passage can exceed 6 m/s at the surface and have been shown to be as high as 3.3 m/s at 3 m above the seafloor (Simon Melrose, pers. comm).

The tides and tidal currents in the upper Bay of Fundy have been simulated using the Finite Volume Coastal Ocean Model (FVCOM) following previous work of Karsten et al. (2008) and Karsten et al. (2012). The model only specifies the tides on the open boundary far from the Minas Passage. The tides and currents are allowed to develop in response to the local bathymetry according to basic laws of physics, conservation of mass and momentum. The model has been validated against tide gauge measurements of surface height and ADCP measurements of tidal currents. Simulations were run to coincide with ADCP deployments for validation purposes. A harmonic analysis of the results of these simulations was used to predict the elevation and currents at the C-POD locations during periods of C-POD deployment.

The flood and ebb tides in Minas Passage have very different dynamics. During the flood tide, the flow must pass around Cape Split (Figure 2), forcing the flow north so that the flood tide is restricted to the northern 2/3 of the passage (there can actually be a weak return flow along Cape Split). This produces a very strong jet of flow in the northern section of the passage. As shown in Figure 3, the FORCE lease area lies on the northern edge of this jet, with strong south-easterly flow through the southern portion of the region that becomes weaker closer to the northern shore of the passage. During the ebb tide, the flow out from the Minas Basin spreads evenly across the entire passage, resulting in lower flow speeds. Maximum speeds can be 1 to 1.5 m/s lower on ebb than flood at locations in the FORCE area.

The local flow is also strongly influenced by the local changes in bathymetry. The shelf that extends from Black Rock through the southern portion of the FORCE test area (Figure 4) creates a region of shallow water and results in strong flow as the tide passes over the shelf (Figure 3). Downstream of the shelf are regions of weaker flow but higher turbulence. Black Rock and other coastal headlands create an active eddy field throughout the region (the wake of Black Rock is visible in Figure 3 - bottom panel). These eddies are especially important during the “slack” periods when they can drive local water speeds above 2 m/s. These eddies also make it difficult to clearly distinguish the change from flood to ebb.

The seafloor of the northern section of the Minas Passage is relatively flat and characterized by erosional trenches and exposed bedrock ridges (Fader, 2009; Figure 4). This region exhibits bedrock covered with a layer of surficial sediment, the product of the last glaciation. Adjacent to the small basalt island east of the FORCE site (Black Rock), gravel and sand bedforms dominate. West of Black Rock, and extending into the FORCE lease area, is a large volcanic shelf; surficial sediment consists largely of boulders, cobbles and gravel atop a bedrock base of basalt (Fader, 2009; Shaw et al., 2012). Sediment mobilization of cobbles, gravel and finer sediments is evidenced by low abundance of sessile epibiota on the seafloor at FORCE (Stewart, 2009; Morrison, 2012). During spring tides, current speeds of up to 1.5 m/s have been detected 0.5 m above the seafloor (Oceans Ltd., 2009). Multibeam sonar surveys of the seafloor (2008-2012) indicate significant near-shore slumping of sand and gravel beds, areas of erosion and other shifts in sediment (pers. comm., Gordon Fader, AMGC).

Envirosphere Consultants Ltd. (2009b, 2010b, 2011b) reported on water quality data for the Minas Basin and Minas Passage, including water temperature, suspended particulate matter (SPM) concentrations and turbidity. Given strong vertical mixing, measures of SPM taken at the surface are likely to be similar with depth (Envirosphere, 2011b). SPM values of about 20 mg/L were observed during the months of February and March, following ice melt, with relative low SPM (<10 mg/L) and NTU (<2) values during July-September. Net sediment transport tends to be from Minas Passage to the east into Minas Basin (Wu et al., 2011).

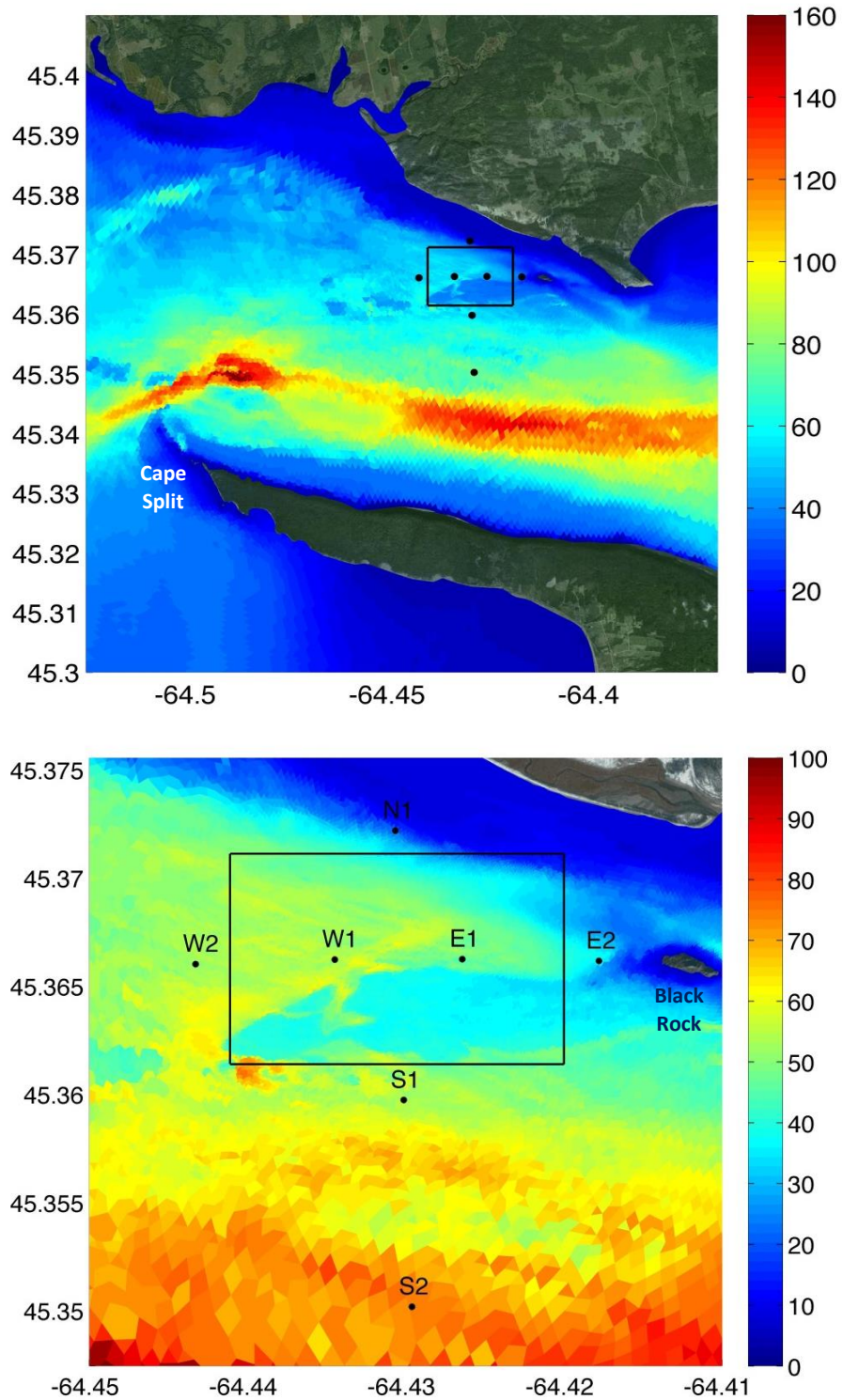


Figure 2. Mean water depths (m) in Minas Passage (top) and the C-POD deployment region (bottom). The locations of the C-PODs are indicated with the black dots; the black box is the FORCE lease area. Note the locations of Cape Split and Black Rock.

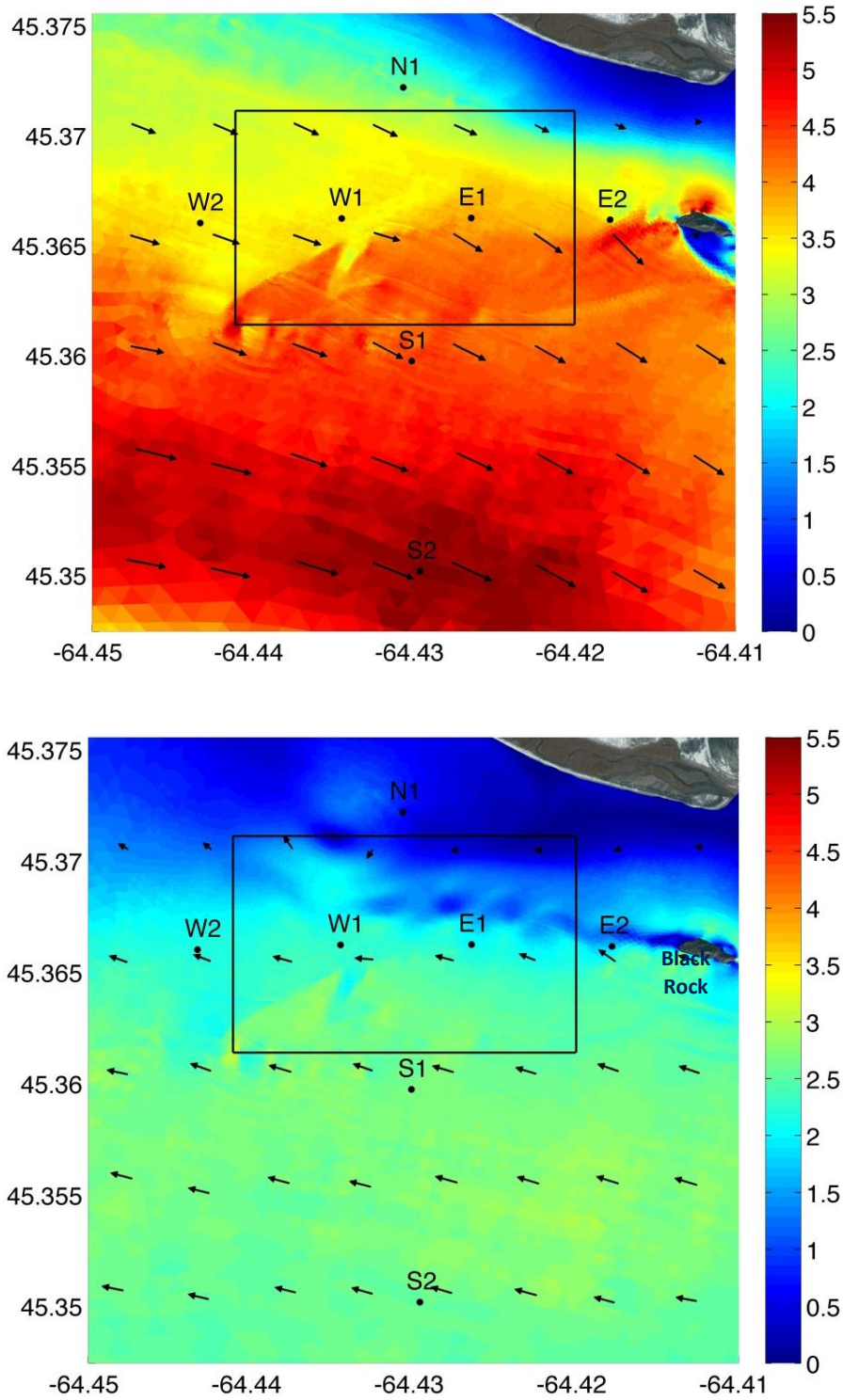


Figure 3. Predicted flow speeds (m/s) and direction in the C-POD deployment region during a typical flood tide (top) and a typical ebb tide (bottom). The arrows indicate the direction of the flow at the given location. The locations of the C-PODs are indicated with the black dots; the black box is the FORCE lease area.

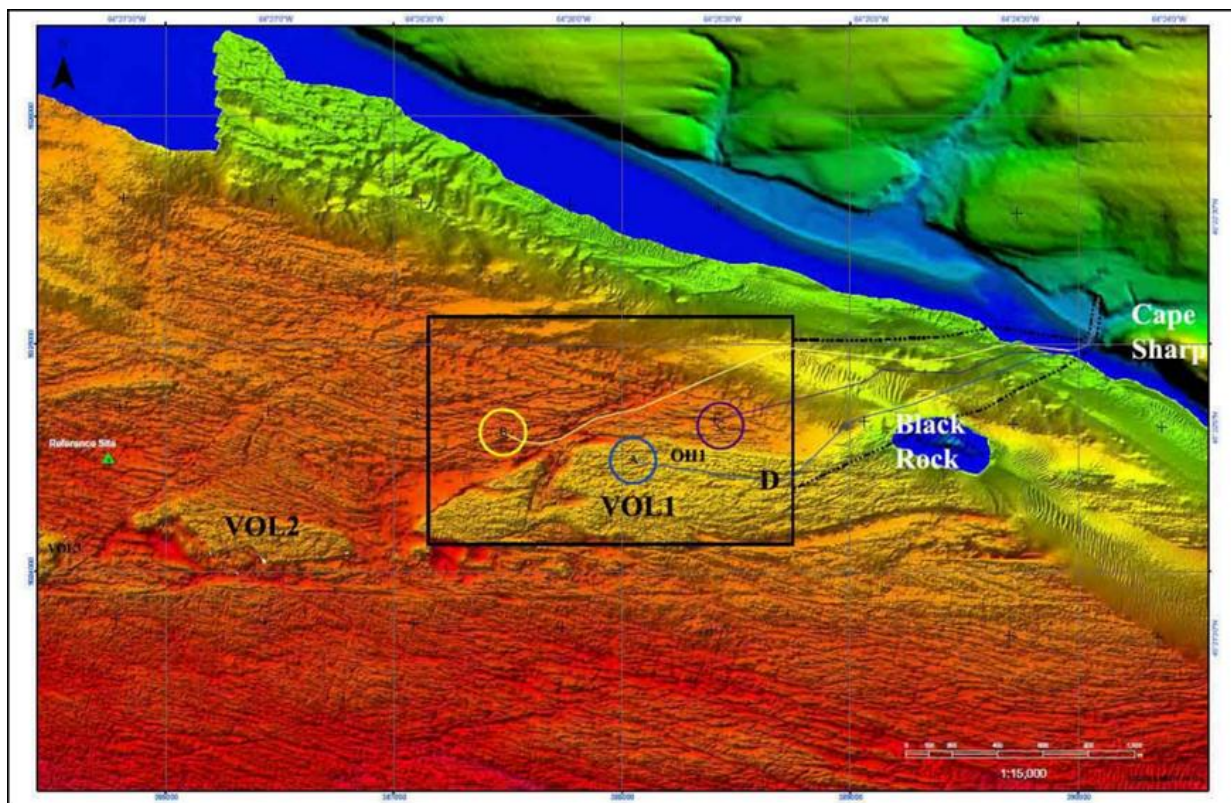


Figure 4. Multibeam bathymetric map of the FORCE test area and surrounds in Minas Passage, Bay of Fundy (Source: GSC, in Fader 2011), showing volcanic platforms (VOL), gravel waves, troughs, and various bedforms. Black Rock is located east of the FORCE site.

3.2 Monitoring Sites

Seven C-PODs were deployed in Minas Passage on 5th May 2011 in a gradient design with two units within the FORCE lease area (W1 and E1) and the rest outside of the lease area (see Figure 2). The East-West axis of C-PODS was designed to compare sites of similar depth, but varying distances from the future TISEC devices. The North-South axis covered deeper and shallower areas compared to the turbine site. Not all units were recovered at the end of 2011.

Monitoring results found the highest amount of sediment noise interference at sites E2 and S2. We therefore focused deployments on the remaining 5 locations in 2012. The first two deployments on May 31st and August 1st placed C-POD units at N1, W2, W1, and E1. The final deployment on September 20th included those locations and S1 as well, due to the fact an additional C-POD was recovered, after collecting data for 167 days in total.

3.3 C-POD Description and Specifications

C-PODs are programmed with several settings before being deployed. These settings affect the ability of the units to detect different species, and how long the units will record data before filling the internal memory. These settings need to be tailored to the specific site and species of interest. C-PODs function by detecting clicks from the raw acoustic data and then only storing data on the click parameters. This allows the units to record ~400 million clicks per deployment, something that would not be possible if the raw acoustic data were to be recorded. The main C-POD settings involve a high-pass acoustic filter and a memory limit. The high-pass filter allows for lower frequencies that are not of interest to be filtered out and therefore avoid the added memory usage of recording those unwanted clicks. Memory usage can also be controlled directly by limiting the number of clicks recorded per minute. Previous experience by SMRU Ltd. and others with C-PODS and hydrophones at tidal sites has shown that the strong currents in these areas move sediments, causing sounds that are recorded as clicks by the C-PODs and hydrophones (Bassett, 2010). Sediment noise is low frequency; therefore the default high pass filter setting of 20 kHz was increased in this study to 40 kHz. High pass filter frequencies exceeding 80 kHz are not recommended as they likely decrease the probability of detecting lower frequency dolphin echolocation clicks. Because sediment noise during strong tidal exchanges saturates the units' memory and therefore limits our ability to measure porpoise presence during large tidal exchanges, we experimented with different memory limit settings and deployment durations. Our standard memory setting has been 4,096 clicks per minute. The next highest setting is 65,536 clicks per minute. We used the standard 4,096 setting during all deployments in 2011. We increased this memory setting to 65,536 for the first two deployments of 2012 which were month long deployments as it was expected that memory capacity would be exceeded in a shorter time period given the larger number of clicks being recorded. We reverted back to a memory setting of 4,096 for the final deployment of 2012 (to extend duration into winter). In our analyses we refer to this memory setting as 'click max'. Once memory has saturated during that minute, click recordings cease. We refer to this as 'memory saturation'. The unit does however track the amount of time it is not recording that minute as '% Time Lost'.

3.4 C-POD Deployment and Retrieval Success

C-PODs were deployed by installing the units into custom-fitted bottom moorings with acoustic releases (provided by the Ocean Tracking Network) as follows. The C-POD was attached to a Teledyne Benthos 875-T shallow water acoustic release and then these units were attached to a modified SUB B3 streamlined instrument buoy (Open Seas Instrumentation, <http://www.openseas.com/>). The Teledyne acoustic release arm was attached to a 3/8" galvanized steel riser chain. During all deployments, except for the first two of 2012, this riser height was 2 m. During the first two deployments of 2012 this riser height was increased to 3

m. The entire unit, weighing 200-220 kg per mooring, included anchors made of 2" diameter steel chain links (Figure 5). Deployments were carried out by ACER personnel using a chartered commercial fishing vessel (Cape Rose) just before high tide in calm conditions.



Figure 5. Rigging units for deployment of C-PODs. Mooring chain weights can be seen on the stern of the vessel. Photo courtesy of Colin Buhariwalla.

Coordinates of deployments are provided in Table 1 and are referenced to surface position of the vessel and not the exact final bottom position of the C-POD unit (estimated to be ± 50 m of release location). Units were deployed as noted in Table 2. Two units were not recovered at the end of the 2011 deployments. One of those lost units was later recovered in the spring of 2012. All units deployed in 2012 were retrieved.

Table 1. Approximate locations of C-PODs deployed in Minas Passage for this study. Depths are at Mean Water Level.

| Location | Latitude | Longitude | Depth (m) |
|----------|-----------|------------|-----------|
| N1 | 45.372180 | -64.430660 | 27 |
| W2 | 45.366010 | -64.443290 | 59 |
| W1 | 45.366220 | -64.434490 | 56 |
| E1 | 45.366240 | -64.426430 | 52 |
| E2 | 45.366160 | -64.417790 | 41 |
| S1 | 45.359730 | -64.430130 | 59 |
| S2 | 45.350170 | -64.429610 | 84 |

Table 2. List of deployments and retrievals by location. Key: 1 The C-POD at location E1 was retrieved early by a lobster fisherman on 24 July, 2011. 2 The C-POD at location E1 was not recovered in December 2011 however it was recovered on 16 June 2012 by a commercial fisher and redeployed during the second deployment of 2012. 3 Two C-POD units were deployed and retrieved at location W1 during the second deployments of 2012.

| Deployment | Deployment Date | Units deployed | Retrieval date | Units Retrieved | Click limit | Riser length (m) |
|------------|-----------------|------------------------------|----------------|--|-------------|------------------|
| 2011 - 1 | 5-May-11 | N1, W2, W1, E1, E2, S1, S2 | 3-Aug-11 | N1, W2, W1, E1 ₁ , E2, S1, S2 | 4,096 | 2 |
| 2011 - 2 | 3-Aug-11 | N1, W2, W1, E1, E2, S1, S2 | 7-Oct-11 | N1, W2, S1, S2 | 4,096 | 2 |
| 2011 - 3 | 7-Oct-11 | N1, W2, S1, S2 | 13-Dec-11 | N1, W2, W1, E1 ₂ , E2 | 4,096 | 2 |
| 2012 - 1 | 31-May-12 | N1, W2, W1, E1 | 1-Aug-12 | N1, W2, W1, E1 | 65,536 | 3 |
| 2012 - 2 | 1-Aug-12 | N1, W2, W1 ₃ , E1 | 20-Sep-12 | N1, W2, W1 ₃ , E1 | 65,536 | 3 |
| 2012 - 3 | 20-Sep-12 | N1, W2, W1, E1, S1 | 4-Dec-12 | N1, W2, W1, E1, S1 | 4,096 | 2 |

3.5 C-POD Data Recovery and Processing

Data was downloaded from the SD memory cards with CPOD.exe V2 software. The Kerno classifier was then used to extract Narrow Band High Frequency (NBHF: in our case, porpoise) and dolphin like click trains from the raw click files. In total there were 1,342 days of data from this two year study. This data was spread through time and location as shown in Figure 6.

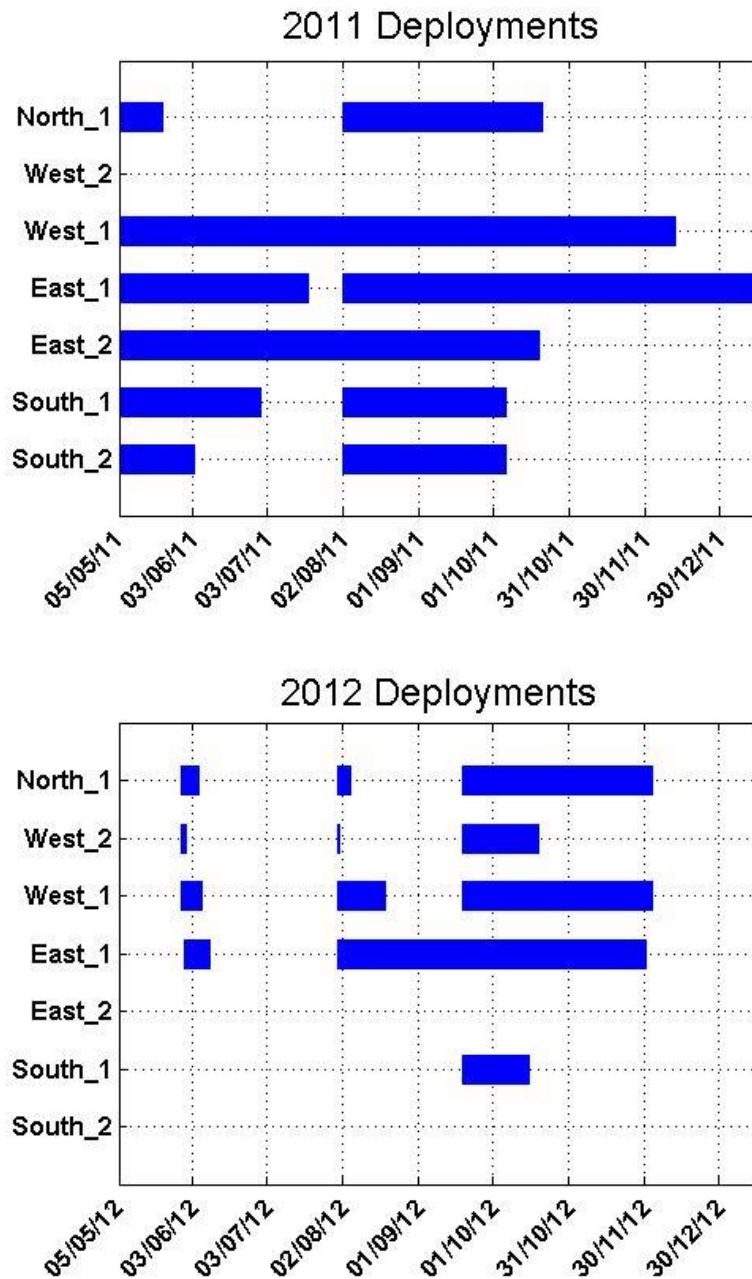


Figure 6. Data retrieved from C-PODs deployed in Minas Passage by location. Top Panel is 2011 data. Bottom Panel is 2012 data. Date format is dd/mm/yy.

Gaps in data are due to either the memory card filling up on the units (occurred during first two deployments of 2012) or an unknown fault in the unit itself. Locations E2 and S2 were not

monitored in 2012 due to unit loss and because these had the worse sediment noise interference.

3.6 Study Plan Variance

Year two of the study varied from year one in the following ways. Sites E2 and S2 were avoided because of their large sediment noise and the loss of two of the 2011 C-POD units. We also changed the first two deployments of 2012 to shorter month long deployments with higher memory buffers to try and better detect porpoise during higher tidal flow regimes. The third deployment reverted back to the longer deployment approach of 2011.

3.7 Data Quality

C-POD software generates warnings on data quality when NBHF or dolphin click rates are low, or when a high proportion of these classified clicks resemble Weak Unknown Transient Signals (WUTS). WUTS can sometimes resemble NBHF or dolphin clicks, but come from other unknown sources (possibly arthropods). These warnings indicate whether NBHF or dolphin clicks need to be verified by a human observer. Due to their low number, all dolphin clicks were verified by hand. Following suggestions by the manufacturer, 100 click trains classified as NBHF by the C-POD software were randomly selected from the data. We estimate from this verification procedure that there is a ~7% false positive rate for NBHF in this data set. Of these incorrectly classified click trains, most were WUTS and a few were sonar.

As discussed in section 3.3, sediment noise is detected by the C-PODs. While it doesn't interfere directly with the unit's ability to detect an echolocation click due to its lower frequency, it can affect the ability to detect porpoise or dolphin clicks by causing memory saturation each minute. 72% of our sampling periods had less than 20% time lost due to memory saturation. The percent time lost varied by location as can be seen in Figure 7. Locations within the FORCE lease area (W1 and E1) are mainly affected by flood spring tides, while location E2 (near Black Rock) is affected at every tidal exchange. This difference between locations is very clear when one compares the cumulative probability distribution of percent time lost at different 2011 locations (Figure 8).

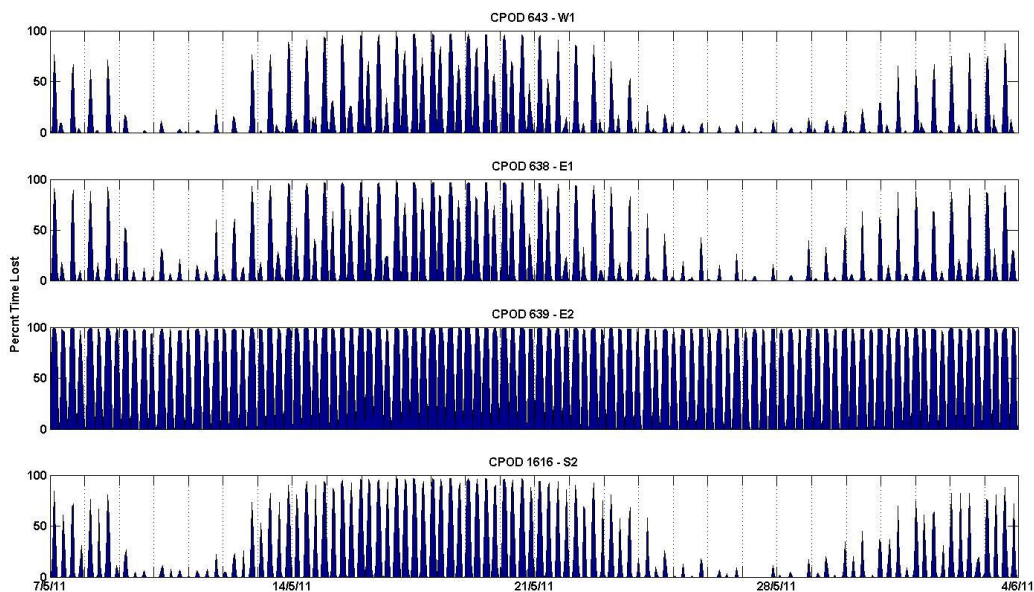


Figure 7. Percent time lost at four locations (W1, E1, E2, S2) during the month of May 2011. Clearly evident are the neap/spring as well as flood/ebb tidal cycles. Locations W1 and E1 are most affected by flood spring tides (and less so by ebb spring). Location E2 is affected at all tidal exchanges, while S2 is affected almost equally on ebb and flood tides during spring exchanges.

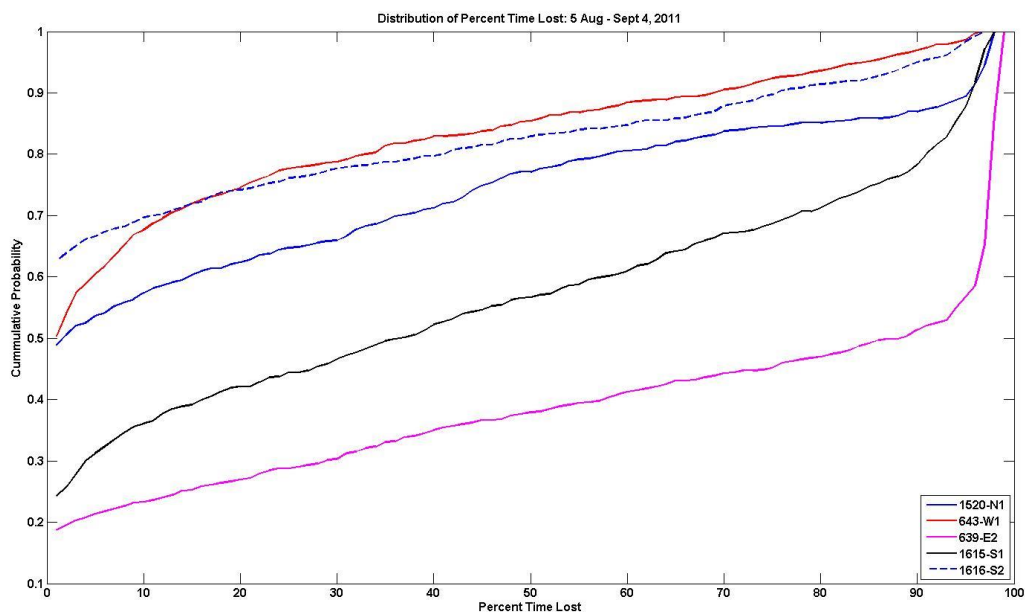


Figure 8. Cumulative probability plot of percent time lost for August 2011 across 5 locations. It is clear that E2 and S1 suffer most from sediment noise.

3.8 Statistical analyses and covariates

For our interim reports (e.g. Tollit et al., 2012) we utilized a negative binomial GLM on each covariate separately (e.g. location, month, etc.) and limited analyses to data with <20% Time Lost. For this final report we used a more sophisticated statistical model that allowed us to model all covariates of interest together and include data with > 20% Time Lost. This amounts to an increase of >33% of data-hours included compared to data included in the interim reports. This was a clear improvement on previous analyses as it allowed us to determine porpoise habitat use during high tidal velocity periods when % Time Lost was high. This more robust and inclusive statistical approach also allowed us to decrease the time scale of C-POD data from detections per hour to detections per 10 minutes and thus to a time scale over which tidal variables are relatively constant. We report descriptive statistics as detection positive minutes per 10 minute period (DPMp10M). C-POD data is temporally auto-correlated at these smaller time scales, non-normally distributed and zero inflated. In order to deal with these issues and produce a robust statistical analysis that incorporated a variety of spatial, temporal and environmental factors, we selected a GAM/GEE modelling approach.

In this analysis, a GAM built within a GEE model construct was used to explain harbour porpoise habitat use across the study site. In order to allow the statistical model to converge DPMp10M was converted to a binary response indicating whether one or more porpoise detection positive minutes occurred in the 10 minute period (1) or not (0), termed DP10M. This binary response was modeled with respect to a range of covariates inside a Generalized Additive Model (GAM) with logit link and binomial error. GAMs have been extremely useful in modeling marine mammal habitat preferences and distribution patterns (Cañadas & Hammond, 2008; De Segura, Hammond, and Raga, 2008; Marubini et al., 2009). However, one of the assumptions of GAM methods is that the model errors are independent. This is not the case with a C-POD dataset as observations are collected close together in time. Therefore, this auto-correlation must be accounted for in the modeling approach, in order for realistic conclusions to be drawn. Because we used a binomial model and there were a large proportion of zeroes in the raw data, it is likely that there will be a very low mean-variance relationship. This may result in underestimation of the uncertainty around model estimates. This was a function of the low detection rates of porpoises.

Generalized Estimating Equations (GEEs) are an extension of Generalized Linear Models (GLMs), facilitating regression analyses of longitudinal data and non-normally distributed variables (Liang and Zeger, 1986; Hardin and Hilbe, 2002). GEEs can be used to account for temporal and spatial auto-correlation within a dataset as they function by replacing the assumption of independence with a correlation structure. Data within the model are grouped into a series of 'panels', within which model errors are allowed to be correlated and between which data are

assumed to be independent. A suitable 'panel' size was chosen using autocorrelation function plots and a simple working independence correlation model structure was also selected. This model structure provides identical coefficients to those of a standard GAM-based approach, but the standard errors will differ significantly under the GEE structure, strongly influencing final model selection results, avoiding the incorrect inclusion of covariates. GEEs have also been used in other circumstances to estimate cetacean habitat preferences from auto-correlated data (Booth et al., 2013; Panigada et al., 2008).

All statistical analyses were conducted using the computer package 'R' (R Core Team, 2012). Within R a series of statistical packages (or programs) are utilised to perform bespoke analyses. The following 'packages' were used here to assess porpoise activity in the Bay of Fundy region: mgcv (Wood, 2011); MASS (Venables and Ripley, 2002); geepack (Hojsgaard, Halekoh, and Yan, 2006); splines (R Core Team, 2012); car (Fox and Weisberg, 2011); mvtnorm (Genz et al., 2012).

3.8.1 Candidate Covariates

A range of environmental, oceanographic and survey (i.e. impacting detection) variables are known to impact studies of cetacean habitat preference (Cañadas and Hammond, 2008; De Segura et al., 2008; Marubini et al., 2009; Skov and Thomsen, 2008). In our statistical models, we included as **candidate** covariates those covariates that helped us to answer our study objectives (e.g. temporal, spatial and tidal covariates) as well as other covariates we thought might impact the ability of a C-POD to detect porpoise (e.g. % Time Lost).

To investigate the potential for differing detection sensitivities between C-POD units, **Pod ID** was included as a covariate in the models as PODs were rotated between sites. The **Location** at which C-PODs were deployed was included to capture spatial/depth differences in the study area. The covariate **Area** was included to test whether detections inside and outside the FORCE test sight differed. **Click max** was also included as a covariate in case this setting had an impact on detection probabilities. To control for sediment noise, **% Time Lost** was included as a candidate covariate.

Previous studies have investigated whether harbour porpoises have diurnal patterns of movement and/or vocalisation behaviour (Akamatsu et al., 1994; Carlstrom, 2005; Todd et al., 2009). To assess whether harbour porpoise exhibit such shifts in Minas Passage, **Day Night Index** was included in the models as a candidate covariate - as a continuous index between 0 and 2, values between 0 (sunrise) and 1 (sunset) indicating day-time and values between 1 (sunset) and 2 (following days sunrise) indicating night-time. This index therefore adjusted for the change of day/night length across the year and is a measure of the % of the day or night that has elapsed. For example an index of 0.5 is halfway through the day (mid-day) and an index of 1.5 is halfway through the night (mid-night).

Seasonal variations in harbour porpoise habitat use have been observed in a number of studies using C-PODs and acoustic surveys (Booth et al., 2011; Verfuss et al., 2007). Consequently, **Julian Day** was included as a candidate covariate to determine if harbour porpoise detections exhibited the same seasonal usage patterns documented by visual observations in other parts of the Bay of Fundy (Neave & Wright, 1968). Julian Day was defined as the day of the year from 1 to 365. Likewise, a relationship between porpoise presence and **temperature** has also been noted in other parts of the Bay of Fundy (Gaskin et al., 1985) and so was included as a candidate covariate.

Porpoise distribution has been associated with state of tide, with animals appearing more prevalent or more detectable during certain phases of tide (e.g. slack, flood, ebb). A range of studies of their distribution have identified site-specific patterns associated with tidal activity (Embling et al., 2010; Johnston, Westgate, and Read, 2005; Pierpoint, 2008; Skov and Thomsen, 2008). In this study we included tidal velocity and tidal height as covariates in our statistical models. The tidal variables we used are not direct measurements but are estimates based on the model simulations discussed in Section 3.1.

3.8.2 Investigating Singularities and Collinearities

When running the initial GAM model, singularities became evident and caused the model to fail to converge. Singularities are caused by only one level of a covariate being present in a single level of another covariate (e.g. a single Pod ID only being present in one location). Pod ID and Area were dropped from the model due to singularities with location (Table 3). Collinearity between covariates, if unaccounted for in models, can cause inflated or underestimated standard errors and p -values and lead to poor model selection. To avoid this, collinearity between predictor variables was investigated prior to modeling using ‘variance inflation factors’ (VIF) (Cox and Snell, 1989; Fox and Monette, 1992) using the *vif* function in the ‘car package’ in R. Large VIF values indicate collinearity and a threshold of $VIF = 10$ was used here. $VIFs > 10$ resulted in the retention of the covariate with the best fit to the data, and the other covariates being removed. Temperature was found to be collinear with Julian Day and was thus dropped from the model (Table 3).

Table 3. List of covariates that were considered in the statistical models and reasons why they were excluded from the final model.

| Candidate Covariate | Retained in Model? |
|------------------------------|---|
| Pod ID | No - due to singularities with pods 1616 and 1880 always being in the same location |
| Location | Yes |
| Area | No - due to singularities with location (only W1 & E1 in FORCE area) |
| Click Max | Yes |
| % Time Lost (sediment noise) | Yes |
| Day Night Index | Yes |
| Julian Day | Yes |
| Temperature | No - due to collinearity with Julian Day |
| Tidal Velocity | Yes |
| Tidal Height | Yes |

3.8.3 Model Selection

A single main model was constructed using all the porpoise data collected from the study area. The type of spline to be fitted, the number and placement of knots within the splines and the overall model selection was conducted using the SALSA package (Walker et al., 2011). As part of this process, GEE-based p -values were used to determine the statistical significance of each covariate and terms with large p -values were removed from the model. The relative importance of each covariate was assessed by looking at the drop in concordance correlation coefficients caused by removing a covariate from the full model. The concordance correlation coefficient combines measures of both precision and accuracy to determine how far the data deviate from a line of perfect concordance. The coefficient increases in value (to 1) as a function of the nearness of the data's reduced major axis to the line of perfect concordance (the accuracy of the data) and of the tightness of the data about its reduced major axis (the precision of the data)(Lin, 1989).

3.9 Data Interpretation and Visualization

Since the GAM/GEE analysis presents overarching modeled trends in porpoise detections, but not actual numbers of porpoise detections, these were computed and provided. In addition, various plots were generated to help interpret the fine-scale trends between porpoise detections and covariates that are occurring in the data.

3.10 Comparing the Performance of Hydrophone Technologies

Another hydrophone technology (icListenHF, Ocean Sonics Inc.) recently commercially available was acquired for the purpose of comparing porpoise detection capabilities. This section highlights the specifications of the icListenHF hydrophone (for comparison, the C-POD specifications are shown in 3.3), range testing of hydrophones in Minas Basin nearshore waters, deployment methodology and data processing. For more details refer to Porskamp (2013).

3.10.1 icListenHF Description and Specifications

The icListenHF hydrophone is a small and compact unit compared to the C-POD (Figure 9, it has a depth rating of 200 m and the detection range (radius) that the manufacturer reports is 1000 m (compared to 300 m for the C-POD). The icListenHF records acoustic signals in the range of 0.01 kHz to 204.8 kHz and can store data in two ways: as Fast Fourier Transform data (FFT files) for creation of spectrum charts or as waveform data (audio files). It can log data internally for short periods or the unit can be attached via cable to a computer (i.e. live feed). Deployments of longer than 1 day require an accessory battery pack cabled to the device. The internal power (lithium) of the icListenHF hydrophone has a life span of just 8 hours when set to record .WAV data. The external lithium battery pack developed for this study enabled FFT data to be recorded continuously for approximately 1 month. For comparison, specifications for the icListenHF and C-POD are listed in Table 4.



Figure 9. Images of a C-POD (top) and an icListenHF hydrophone (bottom). See Table 4 for specifications.

Table 4. Specifications for the icListenHF and C-POD hydrophones used in this study.

| Specification | C-POD | icListenHF |
|--|--|---|
| Length (cm) | 53.5 | 22 |
| Diameter (cm) | 9 | 4.5 |
| Casing Type | Polypropylene | Ultem |
| Depth Rating (m) | 100 | 200 |
| Frequency Range (kHz) | 20-160 | 0.01-204.8 |
| Battery Life - Type | Int. 4-5 months/ 8 alkaline D-cells | Int. 8 hours/lithium Ext. 30 days/lithium pack |
| Memory Capacity – storage location | 4 GB - SD card | 32 GB - internal |
| Operational Range (radius m) * | 300 | 1000 |
| Potential Listening Volume (m ³) | 18 000 000 | 200 000 000 |

*Based on claims of the manufacturer

The icListenHF was configured specifically to process the peak differences in intensity of the acoustic signals received and to update this four times a second (Ocean Sonics, 2012). At these settings, the unit stores about 586 MB of FFT data per 24 hours of data collection. The configuration of the hydrophone and data processing was conducted using the LUCY software program (Ocean Sonics Ltd.), which replays the FFT files as spectrum data in “slow”, “real-time” or “fast” settings (Ocean Sonics, 2012).

3.10.2 Range Detection Tests

The detection ranges of both C-PODS and the icListenHF were tested on the shore of the Minas Basin at Kingsport, NS, which has a gentle slope and substrate of mainly of silt and sand. The range test involved mooring a C-POD and an icListenHF hydrophone. Two Vemco V13 transmitters (69 kHz) were positioned for 2-3 minute periods at 25 m intervals over a 500 m distance from the moored sensors. The icListenHF detected Vemco tag transmissions at the most distant location (500m), which suggests that the detection range exceeded 500 m. The C-POD detected tags up to 375 m from the sensor. The waters of the test environment were calm and represent low ambient noise conditions. Detection ranges are expected to be reduced in naturally noisy environments like Minas Passage.

3.10.3 Mooring Designs for Co-located Hydrophones

Since 2010, all Minas Passage studies involving acoustic monitoring of marine mammals have employed SUB buoys (Open Seas Instrumentation Inc.), a streamlined casing (about 2 m long) with internal floats, that swivels with the current direction. About 200-220 kg of large anchor chain is required to prevent the mooring from moving. SUB buoys are designed to house an autonomous sensor and an acoustic release for recovery. The mooring design used to house C-PODs and the icListenHF hydrophone is shown in Figure 10. A HOBO temperature logger was

attached to the underside of the SUB buoy for continuous recording of water temperature at the depth of sensor deployment (2-3 m above bottom).

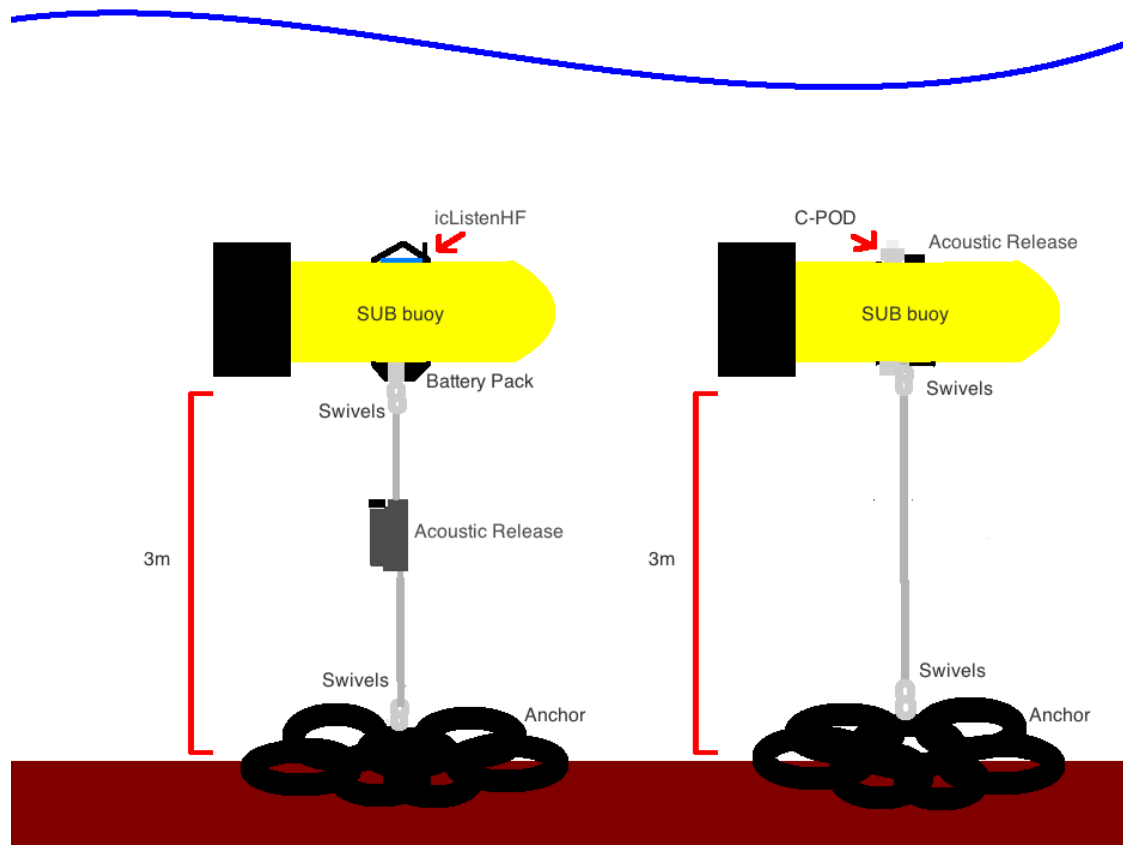


Figure 10. Specialized SUB buoy mooring designs for the icListenHF hydrophone (left) and the C-POD deployments (right). Mooring components shown are not to scale.

3.10.4 Hydrophone Deployment and Retrieval

In preparation for deployment in the Minas Passage, each C-POD was attached to the strongback of a Teledyne Benthos 875-T acoustic release and placed into a SUB buoy that was modified to fit the coupled sensors. On August 1st 2012, three C-PODs and one icListenHF hydrophone were deployed in the FORCE test area from a commercial lobster fishing vessel. The icListenHF was co-located with C-POD 638 and CPOD 639 to facilitate a direct comparison between hydrophones types (Figure 11). All units were retrieved on September 21st 2012 by triggering the acoustic releases.

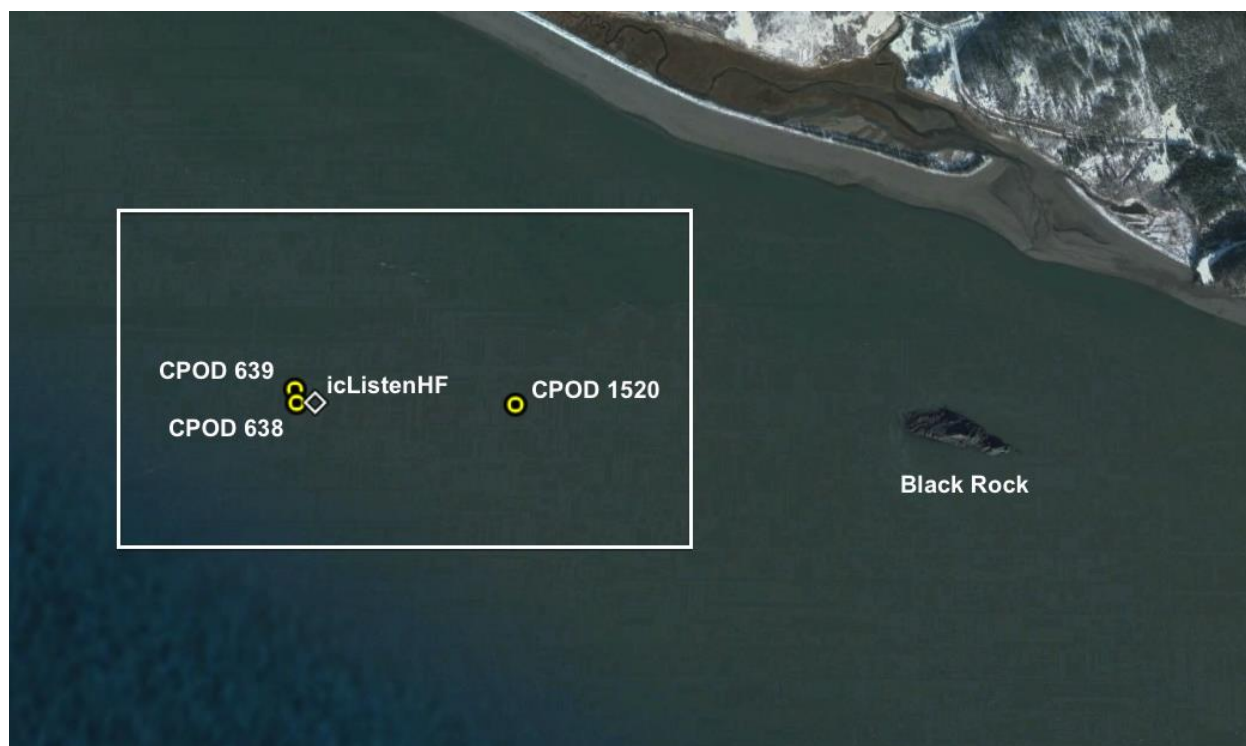


Figure 11. Locations of C-POD and icListenHF hydrophones deployed on August 1st 2012 within the FORCE test site (1 km x 1.6 km).

The memory cards of the three C-PODs deployed in August contained a minimum of 20 days of data (Table 5). The icListenHF hydrophone recorded continuously for nearly 30 days, stopping on August 31st when external battery life expired, as expected.

Table 5. Duration of recording times for all deployed hydrophones. All Hydrophones were deployed on August 1st 2012, at Sites W1 and E1.

| Unit | Site | Recording End Date 2012 | Recording Duration (full days) | % Time too noisy for porpoise click ID |
|------------|------|----------------------------|--------------------------------|--|
| icListenHF | W1 | August 31 st | 29 | 17.5 |
| C-POD 638 | W1 | August 21 st | 20 | 5.4 |
| C-POD 639 | W1 | August 21 st | 20 | 2.9 |
| C-POD 1520 | E1 | September 18 th | 49 | 0.9 |

4.0 RESULTS

4.1 Overall Summary of C-POD Detections

Across the two years of this study a total of 1,342 days (1,932,410 minutes) and a total of 16,065 DPM were recorded at the seven C-POD locations within Minas Passage. There were 397 unique days of monitoring during this study of which only eight had no porpoise detections, thus 98% of days monitored had at least one DPM at one of the locations in Minas Passage. DPM per day ranged from zero to 290. While porpoise were present in Minas Passage on almost every day, they were present on average only 1.5% of the minutes in a day (median DPM/day = 22). Descriptive statistics in 10 minute periods also showed low levels of usage (Table 6).

Table 6. Descriptive statistics for all porpoise data collected in Minas Passage 2011-12. The same metrics are presented in Table 8 through Table 6 to describe porpoise detection results for individual covariates, for ease of comparison. % of 10MP with DPM is the percentage of 10 minute periods with at least one porpoise detection.

| Mean DPMp10M | SD | % of 10MP with DPM | No. of 10MP |
|--------------|------|--------------------|-------------|
| 0.08 | 0.50 | 4.1% | 193,241 |

In contrast, no probable dolphin clicks were detected in Minas Passage during this two year study. Dolphin click detections are more difficult to classify than porpoise clicks because of their larger variation within and between species, and because some of their parameters overlap more with those of other click sources in the ocean (e.g. shrimp). Because there were relatively few dolphin clicks of high quality detected and classified by the C-PODS, these were all verified manually to ensure accurate classification. All of these clicks were false positives with the vast majority being WUTS (Weak Unknown Transient Signals). WUTS are by definition of unknown provenance, but are believed to be biological in origin. Most likely candidates are marine arthropods or fish that are physically in contact with the hydrophone element of the C-POD. One of their most diagnostic features is a steadily increasing Inter Click Interval (Figure 12).

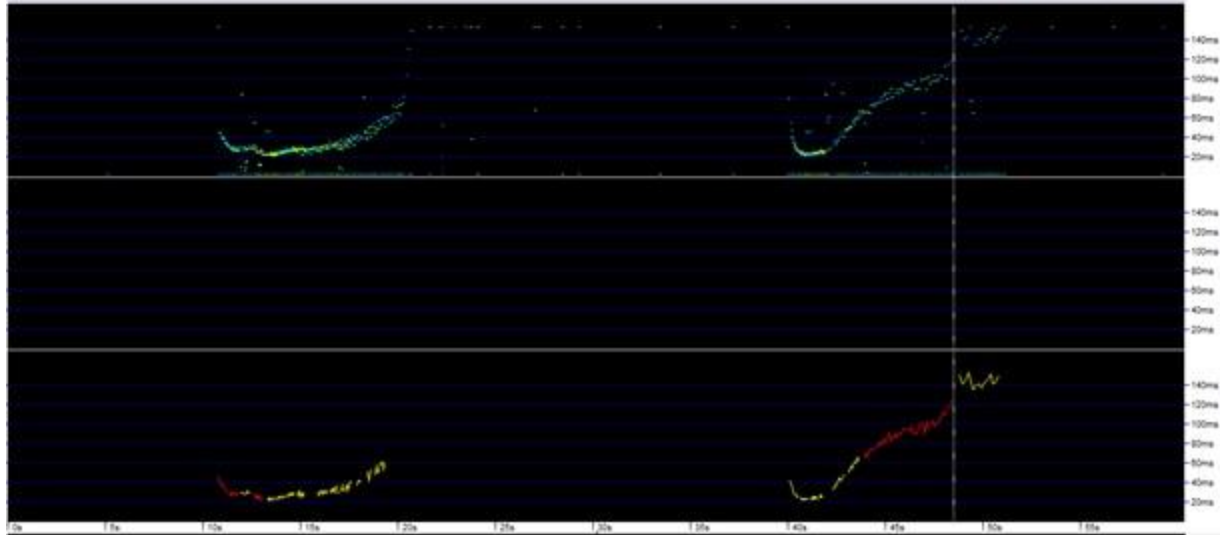


Figure 12. Example of diagnostically increasing Inter Click Interval of Weak Unknown Transient Signals. These WUTS have ICI that increase from 20 to 140 ms over a duration of 10 seconds. Top trace is the raw click detection; bottom trace is the categorized click train. Both of these click trains were erroneously classified as dolphin clicks.

4.2 GAM/GEE Model

Autocorrelation results suggested that a panel size of 120 minutes would provide an adequate time frame for our GEE model. Thus all data within 120 minutes was considered correlated and modelled appropriately by the GEE. Of the seven covariates that were included in model selection (refer back to Table 3), all seven were kept in the final model due to significant (i.e. < 0.05) GEE-based p -values. Concordance correlation coefficients determined that Julian Day was the most important covariate driving porpoise DP10M while Click Max was the least important. Julian Day was considerably more important than any other covariate. Table 7 lists the covariates by rank of importance in relation to porpoise DP10M. The relationship between predictor variables and the response are shown below, also in order of importance (Figure 13). In each plot, the horizontal x-axis is the variable we are interested in investigating the change in porpoise detections with, e.g. time of year or night and day. The vertical y-axis explains how porpoise acoustic activity detection rate changes as the variable of interest (x-axis) changes, but does not depict actual DPMp10M or % of 10MP with DPM. These values are provided in subsequent sections, however the reader should be cautioned that the GAM/GEE model results account for the effects of the other covariates while our descriptive statistics on DPMp10M and % of 10MP with DPM do not. These descriptive statistics are used to depict the magnitude of difference within an **individual** covariate. Mean (SD) are reported, in spite of the data being right skewed and zero inflated, for illustrative purposes and comparison to other studies. Median values of DPMp10M for each covariate are all zero, making comparisons of magnitude challenging. The grey areas around splines and confidence intervals in Figure 13 depict 95% confidence intervals for the predicted relationships (i.e. it is highly likely that the 'true' relationship fits between the upper and lower grey areas). Plots of Julian Day and Day Night

Index (DNI) used circular splines since day 365 is followed by day one and DNI of zero and two are both sunrise. The plot of Julian Day has the start of the year covered with grey hatching to remind readers that, although the spline is fit across this time of year, there is no data for this time of year upon which to base an estimate of porpoise presence.

Table 7. Concordance correlation coefficients (CC) for the significant DP10M covariates retained in the statistical model. Based on these results we were able to rank the importance of each covariate.

| Covariate | Full CC | Covariate CC | Difference in CC | Rank |
|------------------|----------------|---------------------|-------------------------|-------------|
| Julian Day | 0.1129 | 0.0820 | 0.0309 | 1 |
| Tidal Velocity | 0.1129 | 0.0906 | 0.0223 | 2 |
| Tidal Height | 0.1129 | 0.0927 | 0.0202 | 3 |
| Location | 0.1129 | 0.0969 | 0.0160 | 4 |
| DNI | 0.1129 | 0.0979 | 0.0150 | 5 |
| % Time Lost | 0.1129 | 0.0989 | 0.0140 | 6 |
| Click Max | 0.1129 | 0.1127 | 0.0002 | 7 |

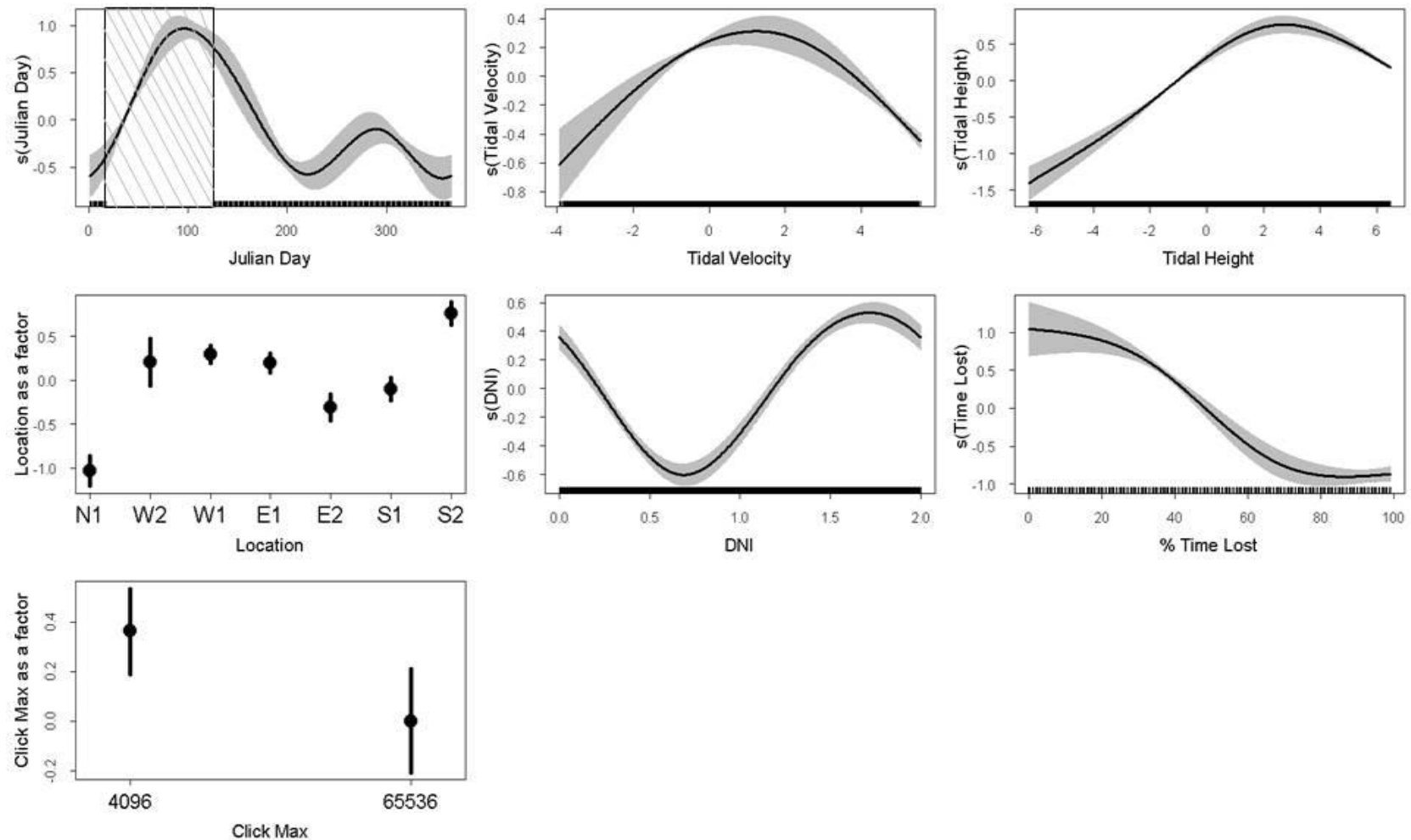


Figure 13. GAM plots of significant covariates and their relationship to porpoise DP10M. Analyses include all data from 2011 and 2012. Plots are in order of importance in predicting porpoise DPM from top left to bottom right. Greyed areas and error bars represent 95% confidence intervals. Hatch marks at base of figures are rug plots that depict the presence of data. The top left figure of Julian Day has cross hatching during the early part of the year to remind readers that while the spline was fit across this time period, there was in fact no data at this time of year and hence a trend can't be estimated during this period.

4.2.1 Julian Day

The GAM plots show the largest peak in porpoise activity occurs in the spring (May) followed by a smaller peak in the fall (late October)(Figure 13). A trough in porpoise detections occurs during the summer (July-August). In terms of mean DPMp10M, the spring peak is approximately double the fall peak, which in turn is approximately double the summer trough (Table 8).

Table 8. Descriptive statistics for periods of 30 Julian Days corresponding to the spring and fall peaks and summer trough in Figure 13. % of 10MP with DPM is the percentage of 10 minute periods with at least one porpoise detection.

| Julian Day Range | Mean DPMp10M | SD | % of 10MP with DPM | No. of 10MP |
|------------------|--------------|------|--------------------|-------------|
| 125-155 | 0.13 | 0.60 | 6.5% | 26,134 |
| 210-240 | 0.03 | 0.28 | 2.0% | 33,080 |
| 280-310 | 0.07 | 0.46 | 3.5% | 30,150 |

Figure 14 depicts the DPM per day split across the two years of this study. While sampling was low in the spring of 2012, there is a clear peak in the spring of 2011 followed by a fall peak in both 2011 and 2012. This plot also shows that while the general pattern of spring/fall peak with summer trough holds across years, the magnitude of peaks may change across years. Seasonal patterns for sites W1 and E1 (within FORCE turbine test area) were similar except during the fall period when DPM/day was often higher at W1 than at E1, during both years of study.

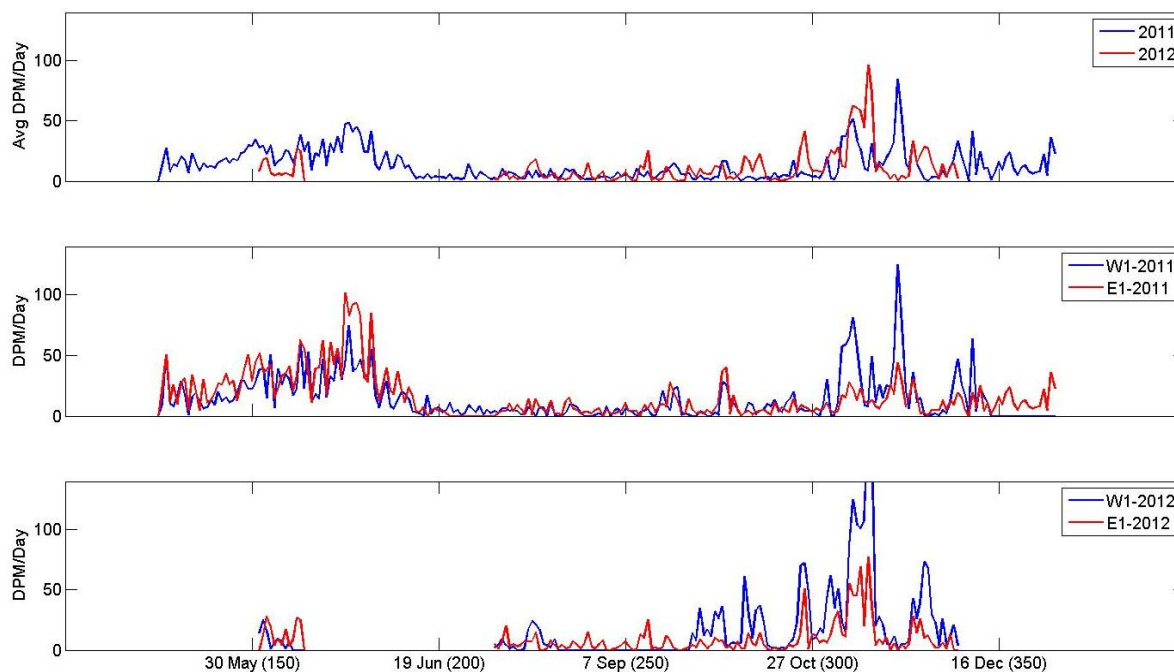


Figure 14. DPM per day in Minas Passage. Top trace is the average DPM per day (averaged across locations being monitored). Middle and bottom traces are DPM per day at the two FORCE locations (W1 and E1) in 2011 and 2012, respectively. Dates are given on the x-axis along with their corresponding Julian Day in parentheses.

Predictions of porpoise detection increase with an increasing flood current until they peak at around 1.8 m/s and then decline again at higher flood velocities (Figure 13). However, on ebb tides, porpoise detections decrease with increasing tidal velocity. Descriptive statistics suggest a very different pattern, with moderate ebb tides having approximately three times the mean DPMp10M of other tidal velocity classes (Table 9). As mentioned in section 4.2 this disparity is likely due to our GAM/GEE model taking account of the effect of the other significant covariates before estimating the effect of tidal velocity on porpoise detections. Data collection on flood currents between 2 and 4 m/s was higher than on ebb currents of 2 to 4 m/s because flood velocities in Minas Passage tend to be higher than ebb velocities.

Table 9. Descriptive statistics for four Tidal Velocity classes. % of 10MP with DPM is the percentage of 10 minute periods with at least one porpoise detection.

| Tidal Velocity (m/s) | Mean DPMp10M | SD | % of 10MP with DPM | No. of 10MP |
|----------------------|--------------|------|--------------------|-------------|
| -4 to -2 (ebb) | 0.06 | 0.40 | 3.4% | 19,102 |
| -2 to 0 (ebb) | 0.15 | 0.69 | 7.0% | 67,105 |
| 0 to 2 (flood) | 0.05 | 0.37 | 3.0% | 56,216 |
| 2 to 4 (flood) | 0.04 | 0.35 | 1.8% | 48,877 |

4.2.2 Tidal Height

According to our GAM/GEE model, porpoise detections are lowest during low tides and highest at moderate high tides (Figure 13). However, descriptive statistics on this covariate alone suggest a continuous increase in porpoise detections from the lowest to the highest tides (Table 10). Again this demonstrates the risk of measurements using one covariate without considering the effects of other covariates.

Table 10. Descriptive statistics for five tidal height classes. A tidal height of zero is the mean tidal height in Minas Passage. % of 10MP with DPM is the percentage of 10 minute periods with at least one porpoise detection.

| Tidal Height (m) Relative to Mean Tidal Height | Mean DPMp10M | SD | % of 10MP with DPM | No. of 10MP |
|--|--------------|------|--------------------|-------------|
| -6 to -4 | 0.05 | 0.37 | 2.7% | 28,832 |
| -4 to -2 | 0.06 | 0.41 | 3.3% | 43,172 |
| -2 to 2 | 0.08 | 0.52 | 3.5% | 56,620 |
| 2 to 4 | 0.11 | 0.58 | 5.4% | 36,952 |
| 4 to 6 | 0.13 | 0.60 | 6.4% | 26,739 |

4.2.3 Location

Porpoise detection rates vary across locations with a tendency to follow an increase in detection rate with an increase in depth of the C-POD sensor (Figure 13 & Table 11). This is more true of the GAM/GEE model than the descriptive statistics. Location N1 is the shallowest

location at 27 m, followed by E2 at 41 m. S2 is at 84 m while the rest are clustered between 50 and 60 m depth. The only location that deviates a little from this apparent pattern is S1 which has a slightly lower detection rate than would be expected based on its depth. Data collection success was highest at W1 and E1 (inside the FORCE area) and lowest at W2 due to technical malfunctions.

Table 11. Descriptive statistics for the seven locations used in this study. % of 10MP with DPM is the percentage of 10 minute periods with at least one porpoise detection. Sites in the FORCE lease area are in bold. Depths are provided in brackets after each location.

| Location (depth: m) | Mean DPMp10M | SD | % of 10MP with DPM | No. of 10MP |
|---------------------|--------------|-------------|--------------------|---------------|
| N1 (27) | 0.03 | 0.26 | 1.3% | 26,212 |
| W2 (59) | 0.07 | 0.43 | 4.1% | 4,704 |
| W1 (56) | 0.12 | 0.64 | 5.5% | 48,840 |
| E1 (52) | 0.10 | 0.55 | 4.9% | 54,226 |
| E2 (41) | 0.04 | 0.36 | 1.7% | 24,213 |
| S1 (59) | 0.06 | 0.41 | 3.6% | 21,272 |
| S2 (84) | 0.11 | 0.52 | 6.4% | 13,774 |

4.2.4 Day Night Index

Considering that a Day Night Index (DNI) of 0 and 2 are sunrise and 1 sunset and that 0.5 and 1.5 are half way through the day and night hours, the lowest porpoise detection rates occur just after midday (DNI ~0.65) while the peak porpoise detections occur at a DNI of ~ 1.65 (Figure 13) or the early hours of the morning. Mean DPMp10M for hours during the night are roughly twice the values for the day (Table 4).

Table 4. Descriptive statistics for four Day Night Index classes. % of 10MP with DPM is the percentage of 10 minute periods with at least one porpoise detection.

| Day Night Index (DNI) | Mean DPMp10M | SD | % of 10MP with DPM | No. of 10MP |
|-----------------------|--------------|------|--------------------|-------------|
| 0-0.5 | 0.07 | 0.45 | 3.7% | 51,338 |
| 0.5-1 | 0.05 | 0.36 | 2.9% | 51,583 |
| 1-1.5 | 0.10 | 0.57 | 4.5% | 45,168 |
| 1.5-2 | 0.12 | 0.62 | 5.5% | 45,152 |

4.2.5 % Time Lost

As % Time Lost increased, porpoise detections decreased, as might be expected (Figure 13 & Table 5). Porpoise detections within the first 25% Time Lost showed little decrease in detection likelihood, however greater than 25% Time Lost led to significant reduction in porpoise detections, with an order of magnitude drop in mean DPMp10M from 0-25 to 50-75 % Time

Lost classes. Overall, a low amount (<25%) of Time Lost was observed in 73% of 10 minute periods, while 18% of 10 minute periods had considerable amounts (>75%) of time lost.

Table 5. Descriptive statistics for four % Time Lost classes. % of 10MP with DPM is the percentage of 10 minute periods with at least one porpoise detection.

| % Time Lost | Mean DPMp10M | SD | % of 10MP with DPM | No. of 10MP |
|-------------|--------------|------|--------------------|-------------|
| 0-25 | 0.11 | 0.58 | 5.4% | 141,730 |
| 25-50 | 0.03 | 0.29 | 1.7% | 8,169 |
| 50-75 | 0.01 | 0.15 | 0.5% | 7,902 |
| 75-99 | 0.00 | 0.09 | 0.1% | 35,440 |

4.2.6 Click Max

A Click Max setting of 4096 resulted in higher porpoise detections (Figure 13) which on average were twice the porpoise detections with a Click Max setting of 65536 (Table 6). Factors likely responsible for these differences include the height of the riser used in Click Max deployments (1 m higher for Click Max 65536). Click max settings also represent different deployment periods (i.e. not concurrent), with only two short deployment periods with C-PODs set at a click max of 65536.

Table 6. Descriptive statistics for the two Click Max settings used in this study. % of 10MP with DPM is the percentage of 10 minute periods with at least one porpoise detection.

| Click Max | Mean DPMp10M | SD | % of 10MP with DPM | No. of 10MP |
|-----------|--------------|------|--------------------|-------------|
| 4096 | 0.09 | 0.52 | 4.3% | 176,291 |
| 65536 | 0.04 | 0.32 | 2.4% | 16,950 |

4.3 Data Interpretation and Visualization: Fine-scale Spatial and Temporal Patterns

4.3.1 Seasonal Patterns

While the GAM/GEE model highlights that there are large differences in seasonal porpoise detections in Minas Passage and that there are differences in detections across location/depth, this tells us little about the relative usage across sites. To determine if there might be more wide spread use during different seasons we focused on 2011 data when monitoring was more continuous (Figure 6). For each 10 minute sampling period we calculated and plotted the proportion of locations that had porpoise detections (Figure 15). Since this is dependent on how many locations were being monitored at that time, we also plotted that information. While some caution is needed in comparing periods with drastically different numbers of locations being monitored (e.g. 6 vs. 2 locations since 2 locations will have a higher probability

of both having detections than 6 will), some broad patterns are evident. Figure 15 suggests that during the spring (May-June), there tend to be detections at a larger proportion of C-POD locations than during the summer (August-September). Likewise fall (October-November) has detections across more locations than summer, and may also be spread across more locations than spring. The 2011 mean (SD) of 10 minute periods with porpoise detections during the peaks and lows identified by the GAM/GEE (spring: 6 May-5 June; summer: 29 July-28 Aug; fall: 7 October-6 November) are respectively 0.23 (0.11); 0.22 (0.12) and 0.47 (0.23), which also suggests that the fall usage is widespread but indicates only a minor difference between spring and summer.

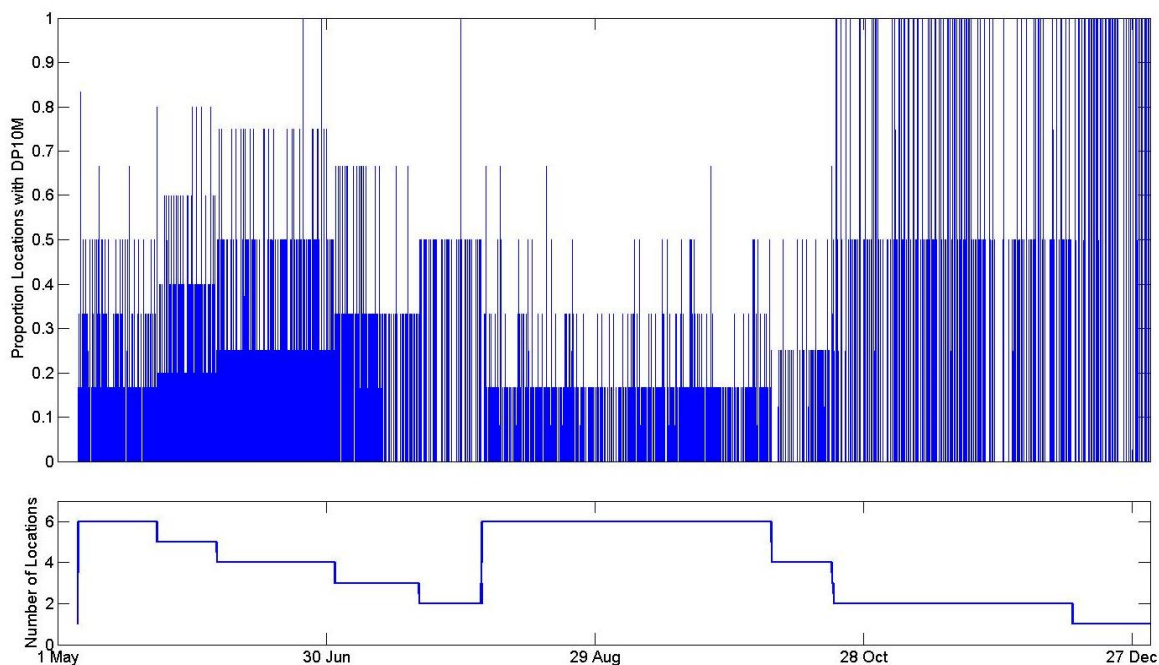


Figure 15. Porpoise detections across locations in 2011. Top trace: proportion of C-POD locations with detections during each 10 minute recording period. Bottom trace: number of locations monitored during 2011.

In addition to describing seasonal trends across locations in Minas Passage, we also assessed trends within a single key site. We selected location W1, which is within the FORCE test area and was the longest continuous monitoring location in 2011. To highlight seasonal trends we present DPMp10M for a month of data during the spring, summer and fall peaks and lows in porpoise detections (Figure 16). There are two main trends evident in these plots across three months. The first is that DPMp10M vary *across* month and are highest in the spring, lowest in the summer and then recover in the fall, just as the GAM/GEE model predicts. The second trend has to do with the regularity of detections *within* each month. Spring has a large number of

peaks throughout this month of data, but those peaks in detection are spread throughout the time period. The summer month has lower detection levels, but is more periodic in when the detections occur. In contrast, the fall month has high usage and very periodic timing in that usage. It does not appear that this is being driven by a spring/neap tidal cycle as these periods had similar tidal ranges (see Figure 17 for the tidal heights during these same periods). Fall peaks are much more clustered around night time (the vertical dashed lines indicated midnight). These differences across seasons may be driven by differences in how porpoise are using this habitat at different times of the year, or by the number of porpoises using this habitat.

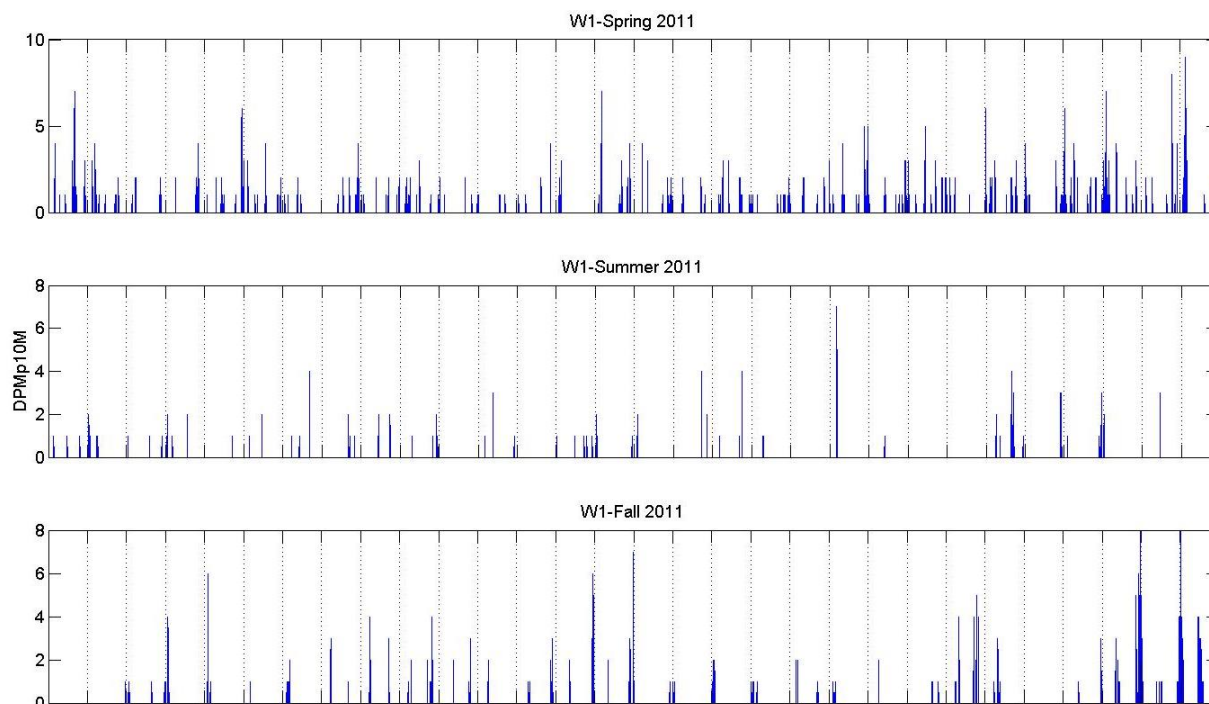


Figure 16. DPMp10M at location W1 highlighting trends across and within month variability. Top trace is spring 2011, middle trace is summer 2011 and the bottom trace is fall 2011. Vertical dashed lines indicate the start of a new day (i.e. midnight).

4.3.2 Tidal Cycle and Diurnal Patterns Inside FORCE

The GAM/GEE model indicated that of the tidal variables Tidal Velocity (average water column velocity) and Tidal Height had the 2nd and 3rd largest impact on porpoise detections. To control for the large impact of season on porpoise detection and focus on tidal variables, we generated a series of tidal plots by season. We chose a subset of data (1 week) to plot in more detail and chose those weeks because of similar tidal ranges (indicated by arrows in Figure 17). For these weeks of data, we then generated separate figures with Tidal Height, % Time Lost, Tidal Velocity and DPMp10M to examine tidal trends in relation to porpoise detections (Figure 18 through

Figure 24). Given that vertical dashed lines indicate the start of each new day (i.e. 0:00) it is also possible to discern trends in time of day effects. The larger seasonal pattern in the number of detections is still evident, however, with a few exceptions, click detections tend to occur at moderate flood tidal velocities, high tides and low % Time Lost, with a smaller correspondence between time of day and porpoise detections. If one were to rank how closely each of these seasons follows tidal and daily patterns, it appears from this data sample that Fall follows the GAM/GEE predictions most closely while summer follows the predictions the least. It is also clear from these plots that flood tides generate more % Time Lost than ebb tides with maximum % time lost occurring at maximum flood tide velocities.

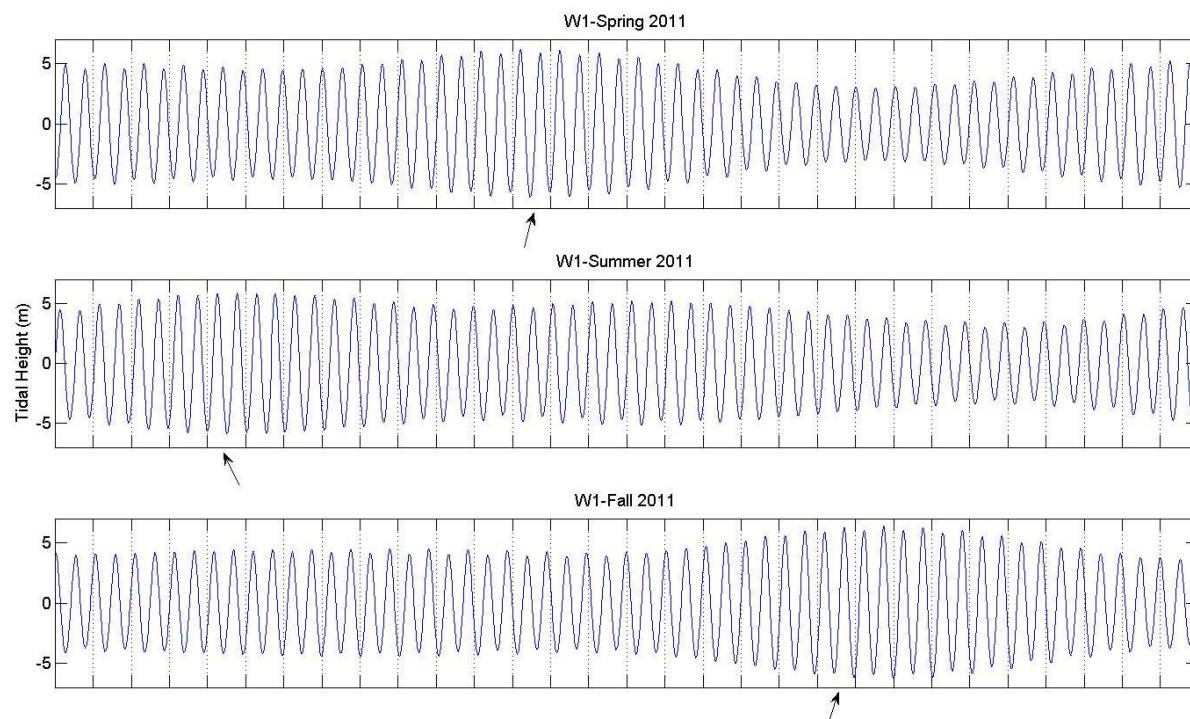


Figure 17. Tidal height (m) across one month periods in the spring, summer and fall. A tidal height of zero is the mean tidal height. Vertical dashed lines indicate the start of a new day (i.e. midnight). Arrows indicate general times where data was extracted from to generate Figure 18 through Figure 24.

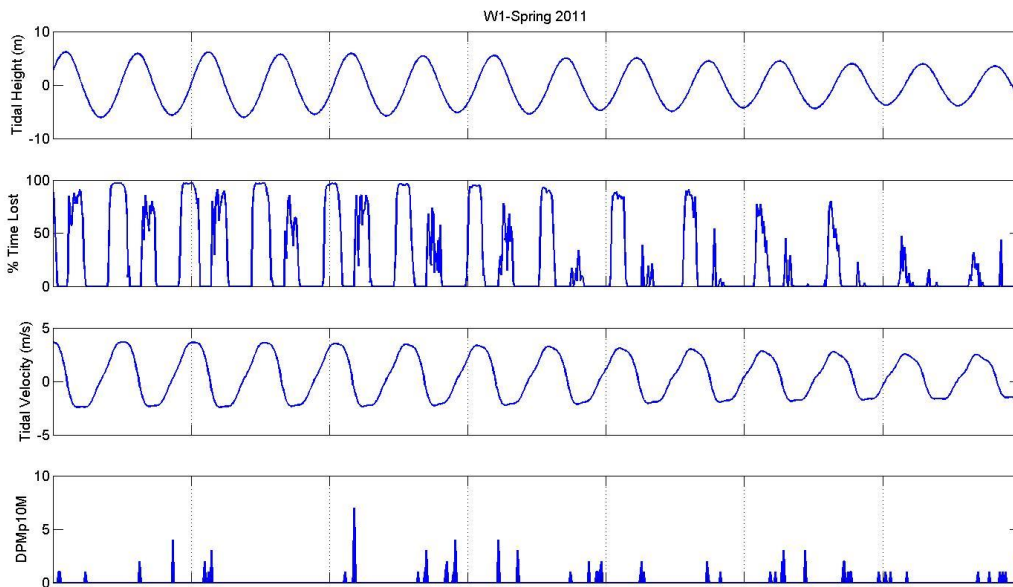


Figure 18. One week of data from W1 during the spring of 2011. Top trace: Tidal height (m); Second trace: % Time Lost; Third trace: Tidal Velocity (m/s); Last trace: DPMp10M. Vertical dashed lines indicate the start of a new day (i.e. midnight).

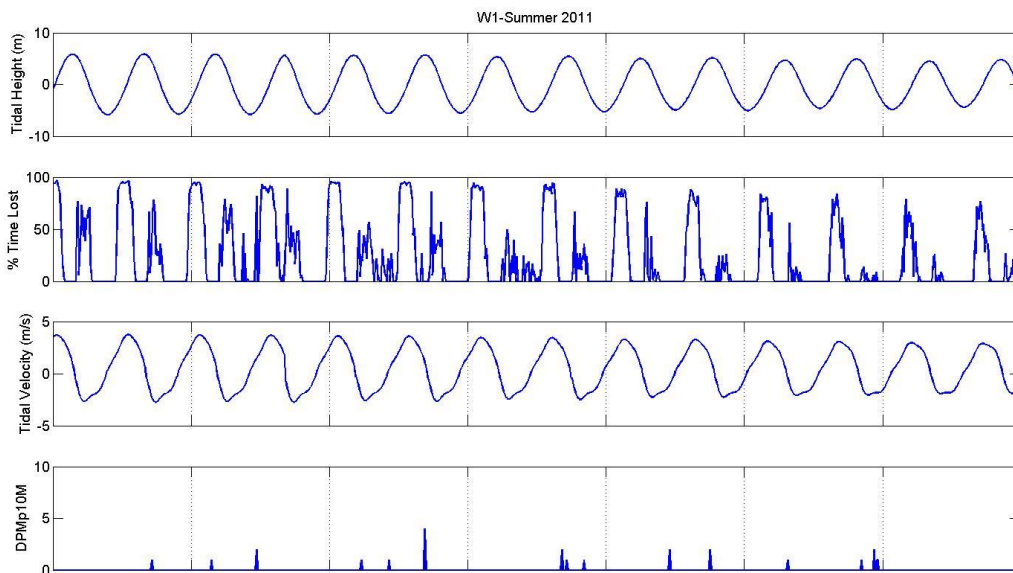


Figure 19. One week of data from W1 during the summer of 2011. Top trace: Tidal height (m); Second trace: % Time Lost; Third trace: Tidal Velocity (m/s); Last trace: DPMp10M. Vertical dashed lines indicate the start of a new day (i.e. midnight).

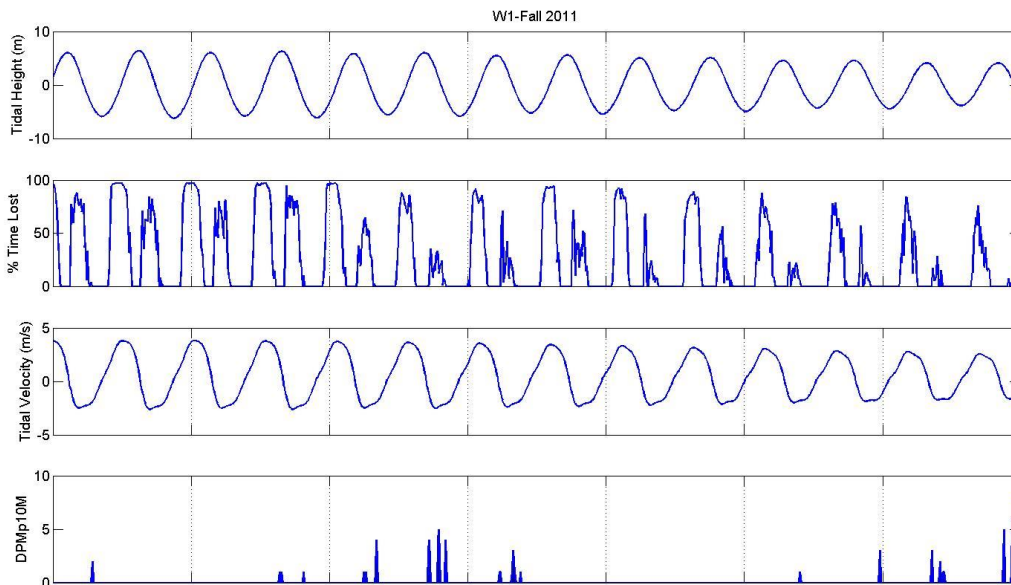


Figure 20. One week of data from W1 during the fall of 2011. Top trace: Tidal height (m); Second trace: % Time Lost; Third trace: Tidal Velocity (m/s); Last trace: DPMp10M. Vertical dashed lines indicate the start of a new day (i.e. midnight).

4.3.3 Tidal Cycle and Diurnal Patterns Outside FORCE

In order to investigate whether the GAM/GEE model trends held at locations outside of the FORCE site; we focused on N1 and S2 due to their large differences in depth. We generated seasonal plots identical to W1 for ease of comparison. However there were no data during the fall of 2011 outside of the FORCE area, so we could not generate those plots. Likewise, to align in time with the data from W1, our spring plot for N1 is missing the last two days of data since the unit stopped recording then. The plots for N1 and S2 in the spring and fall of 2011 show similar trends to W1 inside the FORCE site and seem to be in general agreement with the overall GAM/GEE model predictions (Figure 21 through Figure 24). N1 has fewer detections than W1 in both seasons and S2 has more, as predicted in the GAM/GEE model. Likewise, detections tend to occur most often when the tide is high and % Time Lost is low. Velocity and time of day have a lesser effect.

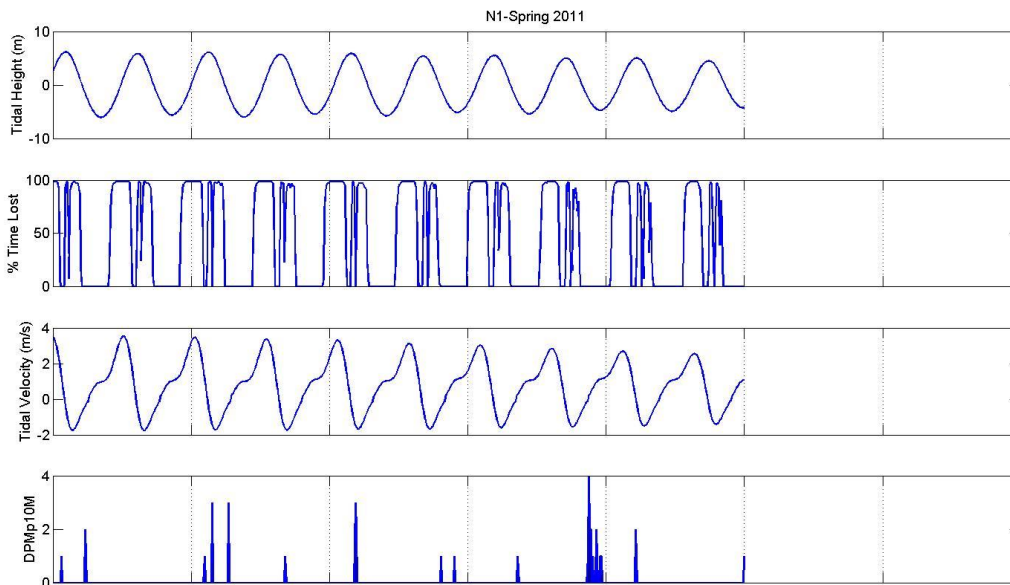


Figure 21. One week of data from N1 during the spring of 2011. Top trace: Tidal height (m); Second trace: % Time Lost; Third trace: Tidal Velocity (m/s); Last trace: DPMp10M. Vertical dashed lines indicate the start of a new day (i.e. midnight). Last two days of data are not depicted due to C-POD not monitoring then.

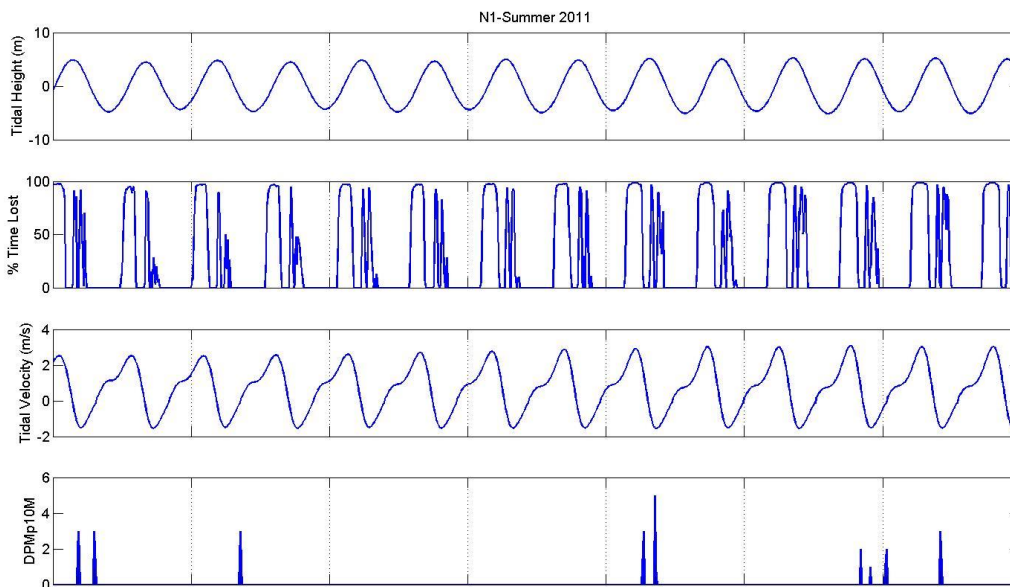


Figure 22. One week of data from N1 during the summer of 2011. Top trace: Tidal height (m); Second trace: % Time Lost; Third trace: Tidal Velocity (m/s); Last trace: DPMp10M. Vertical dashed lines indicate the start of a new day (i.e. midnight).

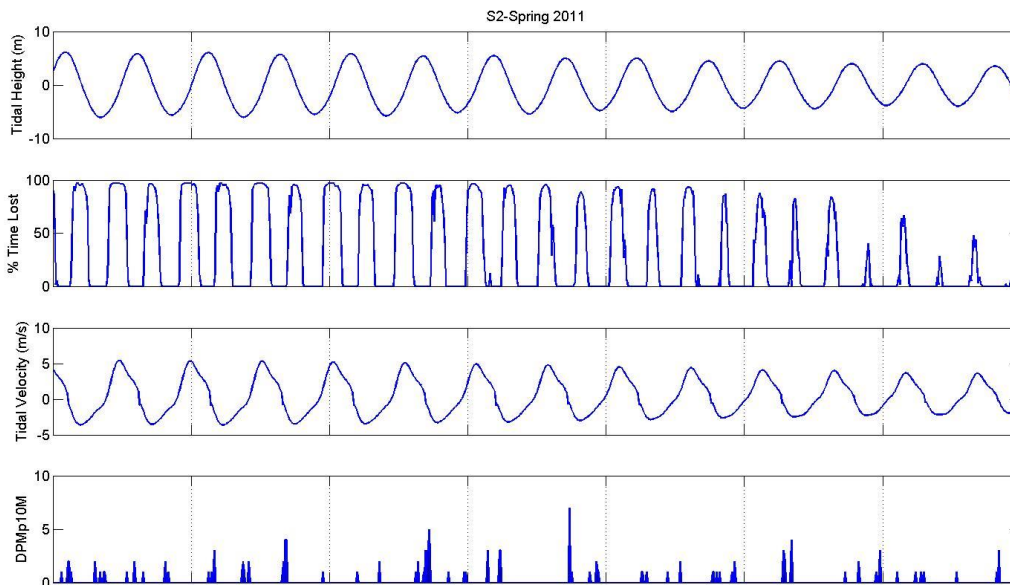


Figure 23. One week of data from S2 during the spring of 2011. Top trace: Tidal height (m); Second trace: % Time Lost; Third trace: Tidal Velocity (m/s); Last trace: DPMp10M. Vertical dashed lines indicate the start of a new day (i.e. midnight).

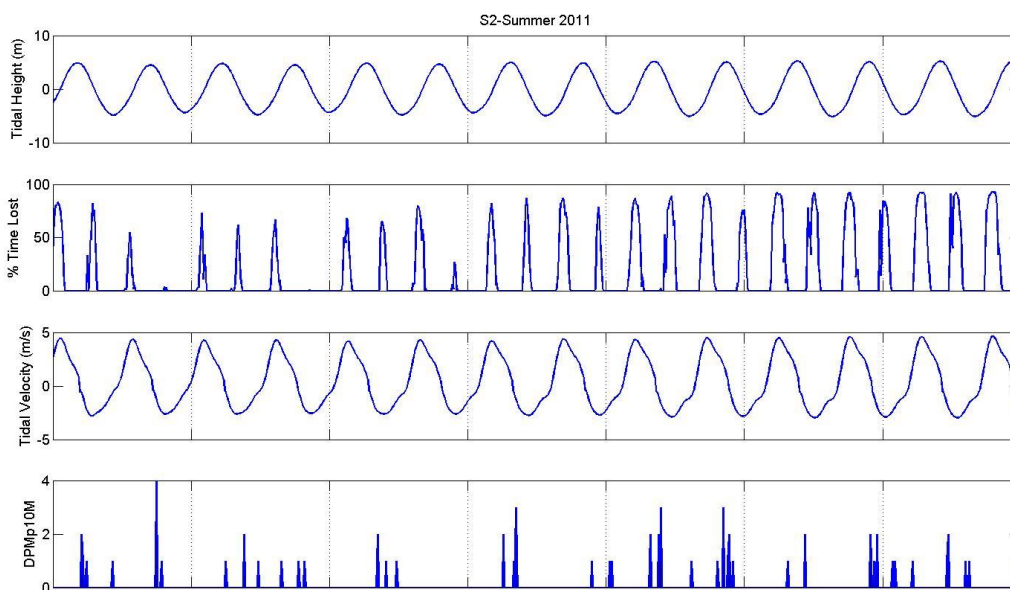


Figure 24. One week of data from S2 during the summer of 2011. Top trace: Tidal height (m); Second trace: % Time Lost; Third trace: Tidal Velocity (m/s); Last trace: DPMp10M. Vertical dashed lines indicate the start of a new day (i.e. midnight).

4.4 icListenHF vs C-POD Porpoise Detections

LUCY software (Ocean Sonics Ltd.) was used to display icListenHF hydrophone FFT data in a spectrum chart as shown in Figure 25. A click train was recognized when the spectrum chart showed decibels of at least 110 dB re 1 μ Pa in the frequency range of 100-130 kHz. Detections per minute were determined by counting the number of individual porpoise detection events in one minute. Information that indicates the presence of a porpoise is backed up by a frequency increase on the frequency response graph located above the FFT graph (Figure 25).

4.4.1 Comparison of Lost Recording Time

Lost porpoise recording time was assessed (at per minute intervals) during the visual processing of each minute of the 29-day set of icListenHF FFT files. A lost minute of recording time is shown when the entire spectrum chart exceeds 140 db re 1 μ Pa at all frequencies. Lost recording time for the icListenHF can occur under high flows when the overall noise (moving bedforms, noise effects of the mooring under strain, etc.) is extreme (i.e. high decibels) and masks any detection of porpoise click trains, if present at the time (Figure 26).

During spring tides the icListenHF recorded noise levels that were often too high to detect porpoise click trains, if any. On each spring tidal cycle, at least 3 hours of recordings were lost due to very high sound levels, especially during the flood tide (Figure 26). During neap tides, when current speeds were slower, there was less noise (ambient plus flow noise around the sensor), and thus little interference with icListenHF detection of click trains, except during the mid-flood period of neap tidal cycles (Figure 27).

The percentage of lost recording time per day for both hydrophone types increased as the tidal range increased and was at its lowest during the neap tide on 12 August (approximately 7 m tidal range). During August 2012, time lost for the icListenHF was in the range of 20-27% during spring tides compared to <12% for C-PODS (Figure 28).

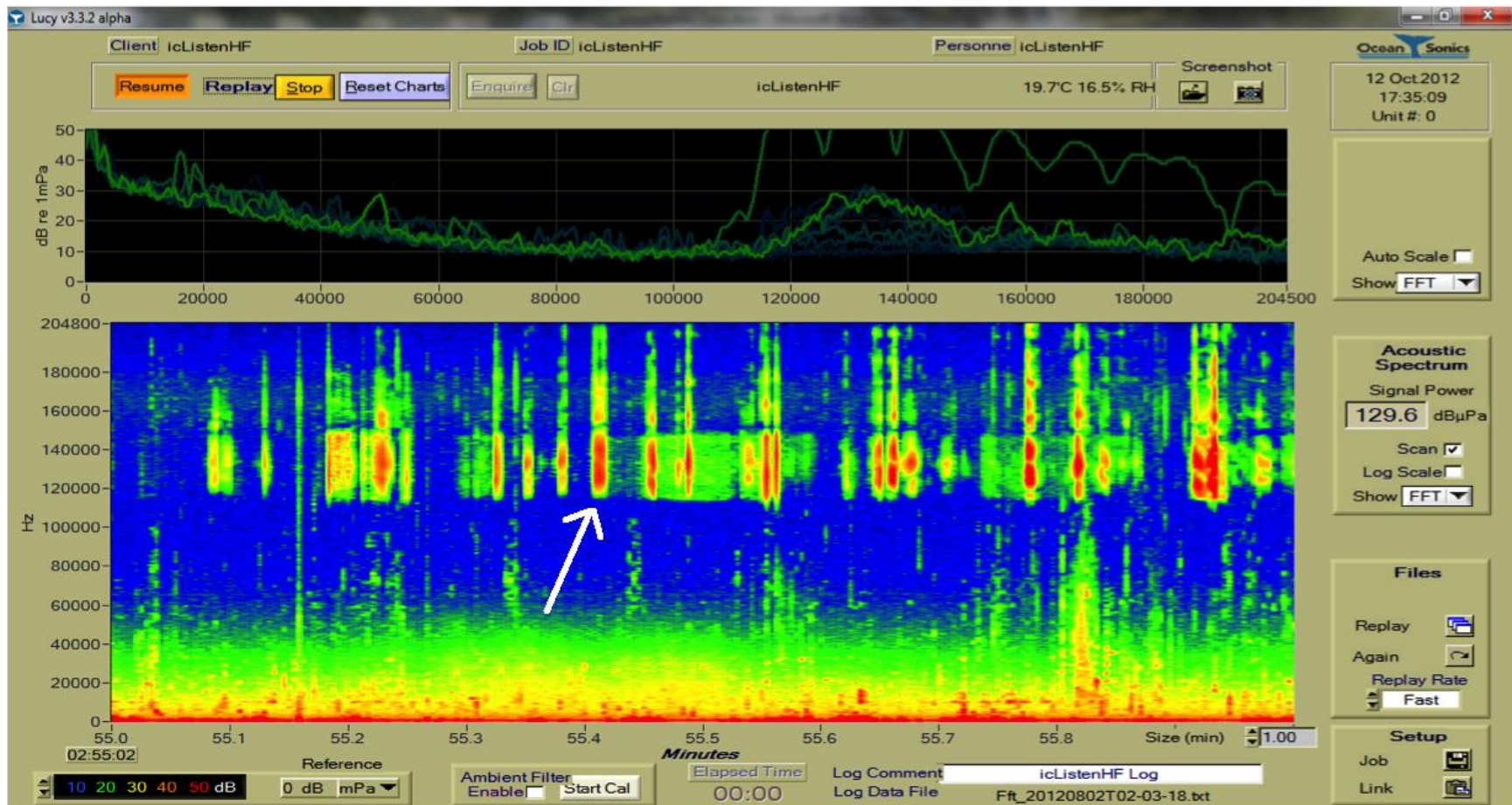


Figure 25. LUCY screenshot showing multiple porpoise click trains within a single minute on August 2nd 2012. White arrow points to a loud individual click train, indicating the porpoise is close to the icListenHF. Time is represented on the x-axis and frequency on the y-axis. The colours represent the amplitude of the sound, blue being low and red being high. The green and yellow colours in the lower frequencies are likely due to sediment noise. Each green line on the response graph (above) represents a 1 second timeframe as the FFT file scrolls to the right.

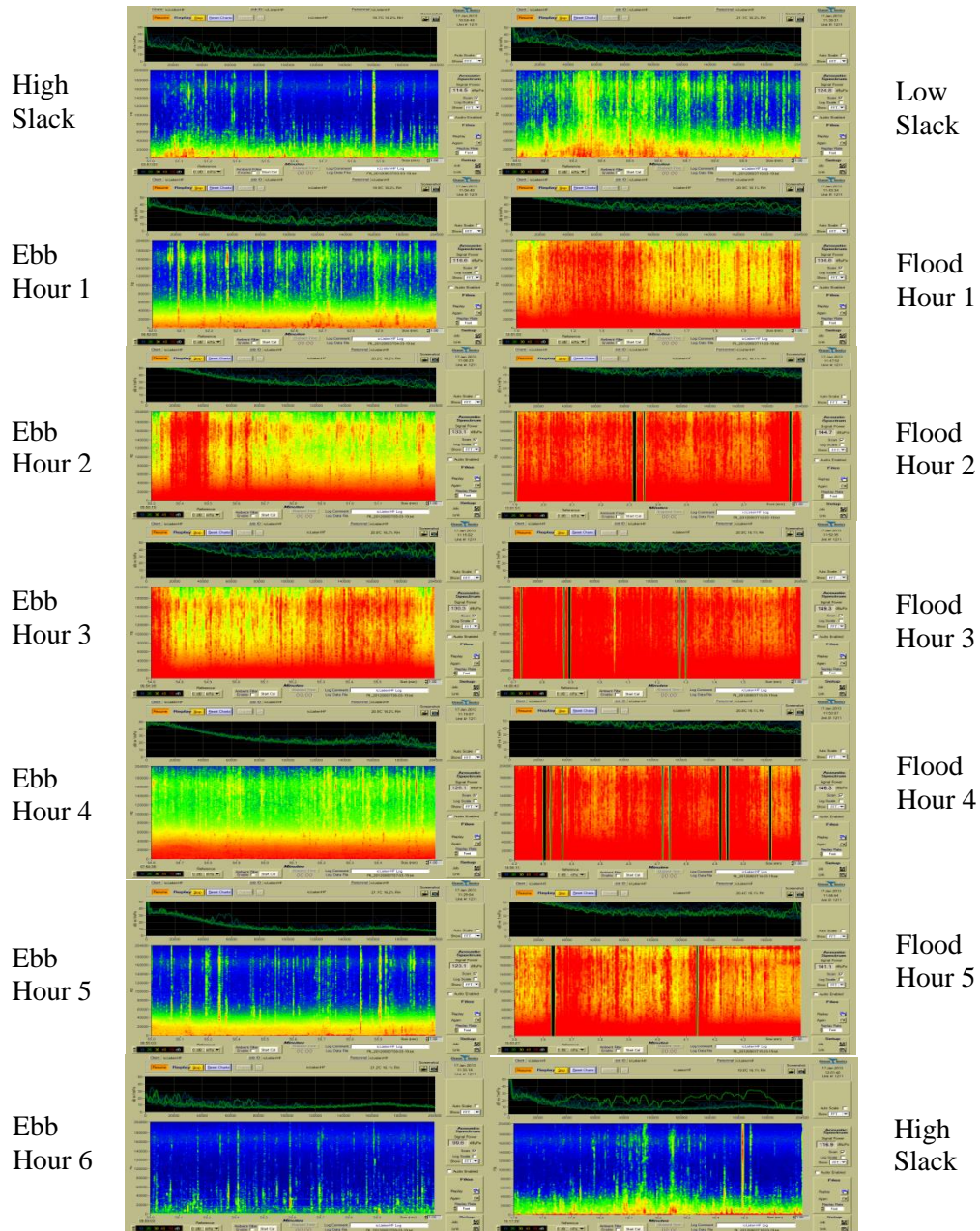


Figure 26. Ebb and Flood tide series of LUCY screenshots (one-minute frames) during a spring tidal cycle on August 3rd 2012. Note the differences in ambient noise during ebb and flood periods.

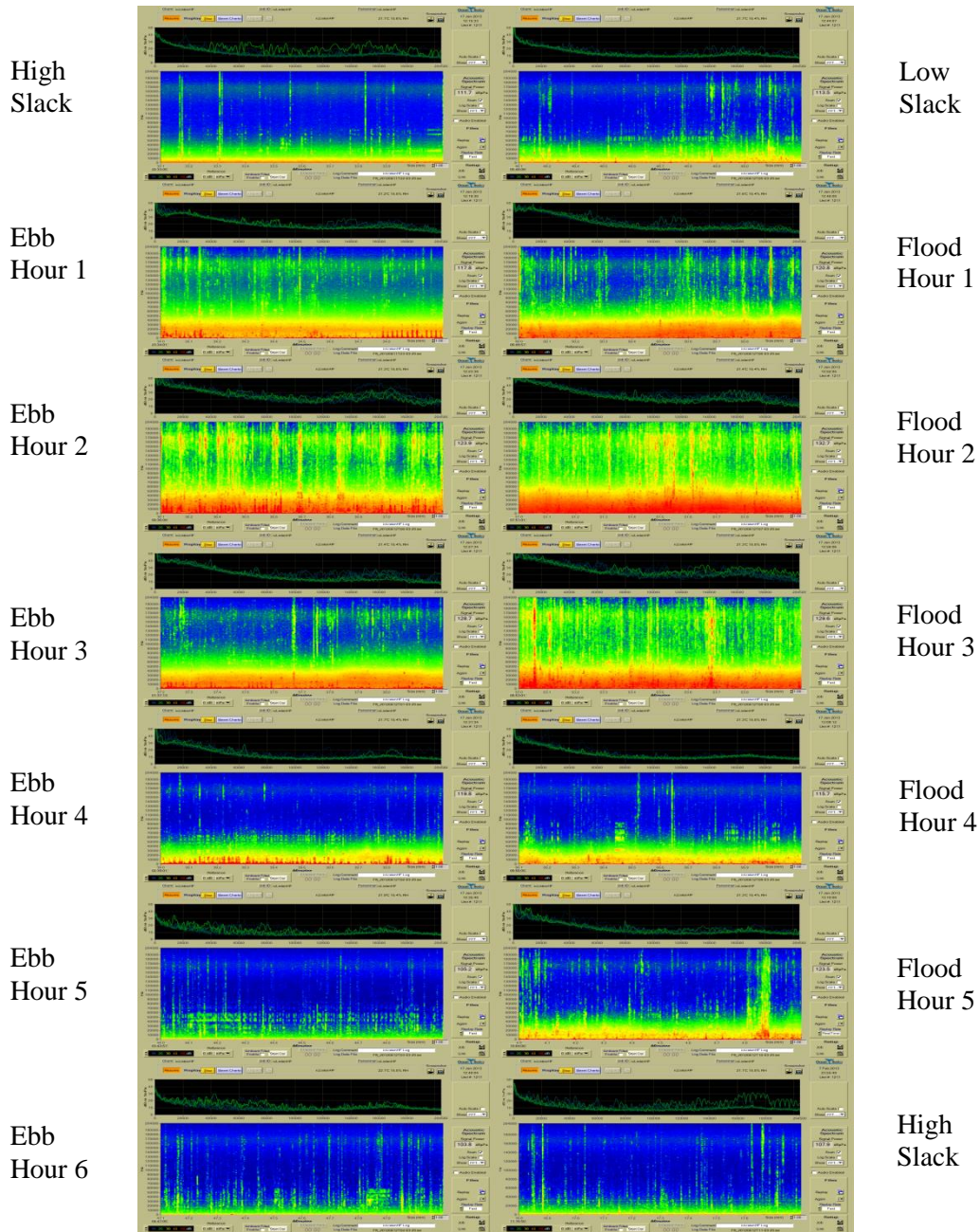


Figure 27. Ebb and Flood tide series of LUCY screenshots (one-minute frames) during a neap tidal cycle on August 11th 2012. Ambient noise levels are lower than those during a spring tide (see Figure 26).

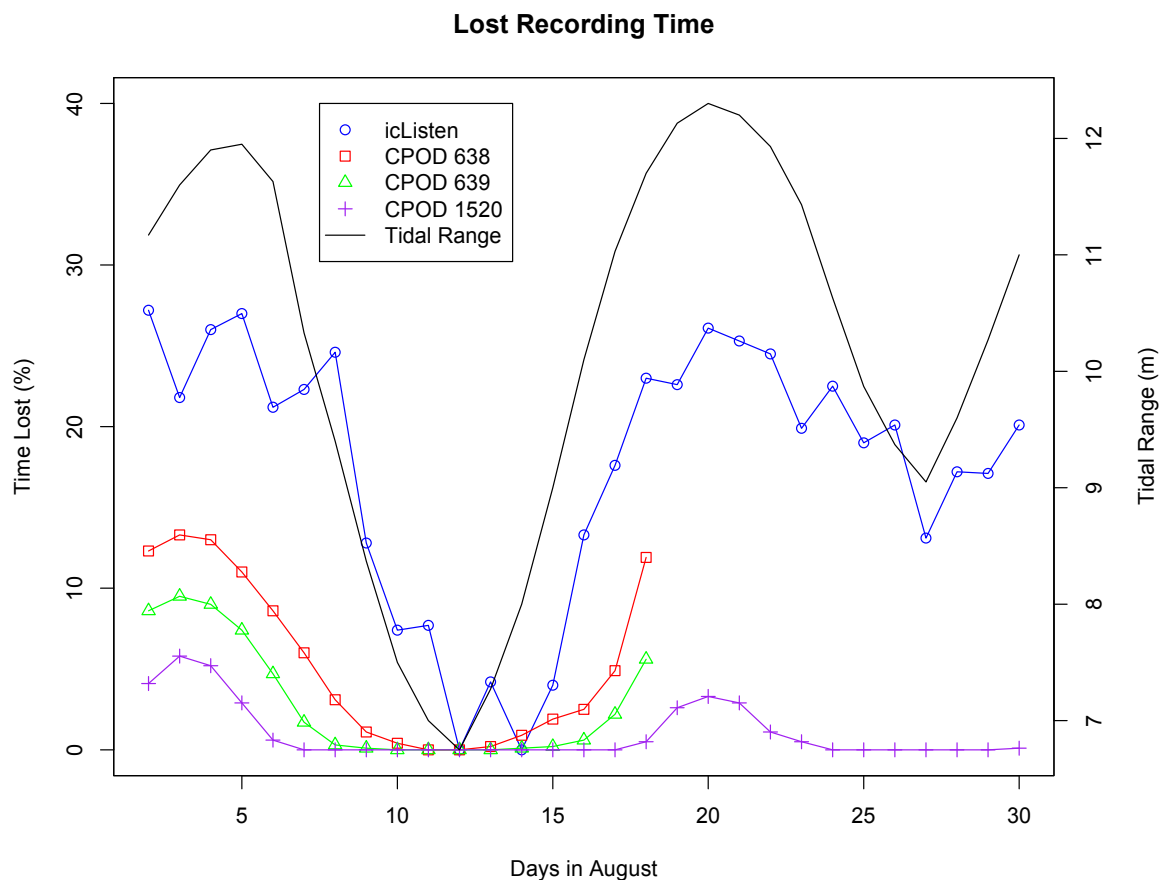


Figure 28. Tidal range and percent lost recording time per day in August 2012 for C-PODs 638, 639, 1520 and icListenHF.

Detection Positive Minutes (DPM) per day and % lost time for the icListenHF are plotted with tidal range in Figure 29. DPM per day varied over the month of August 2012, with peaks in detections of porpoises observed at approximately 3-5 day intervals. The maximum DPM/day occurred during the main neap tidal cycle on August 12th, when % lost time was nil.

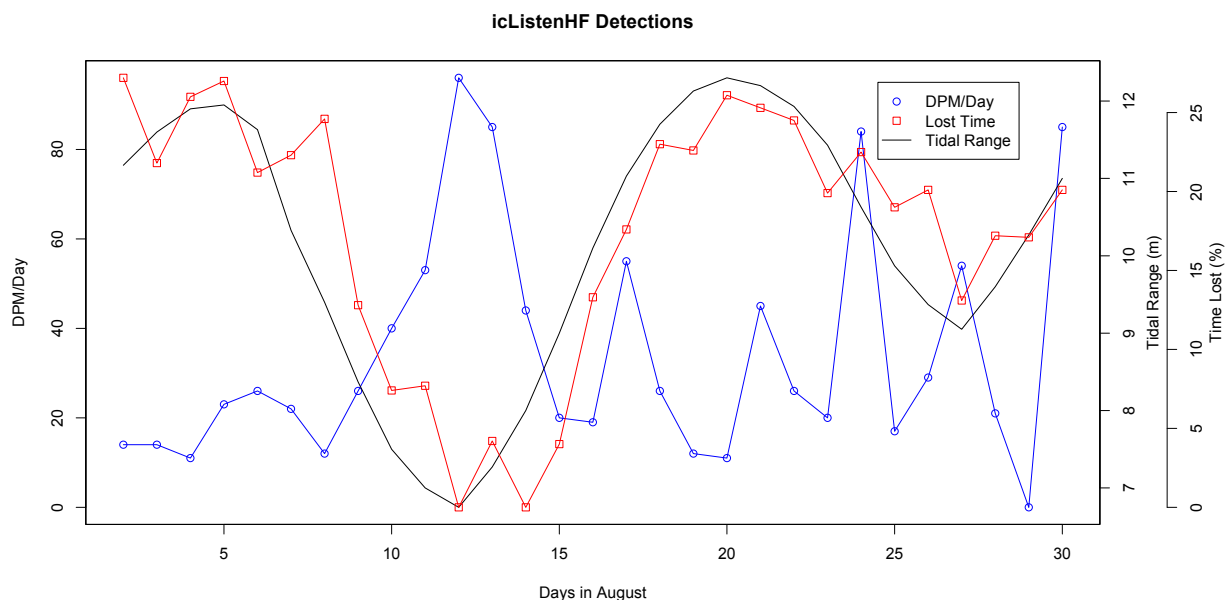


Figure 29. DPM per day, tidal range and percent lost recording time for the icListenHF during the month of August 2012. Water temperature at the depth of the sensors ranged from 15-18 °C during the deployment period.

For all three C-PODs, % lost recording time per day during August 2012 increased exponentially with tidal range (Figure 30). In contrast, the icListenHF showed a linear increase in lost recording time as tidal range increased. Interestingly, there was no loss of recording time for C-POD 1520 at tidal ranges below 11 m. This unit was located about 500 m east of the other hydrophones.

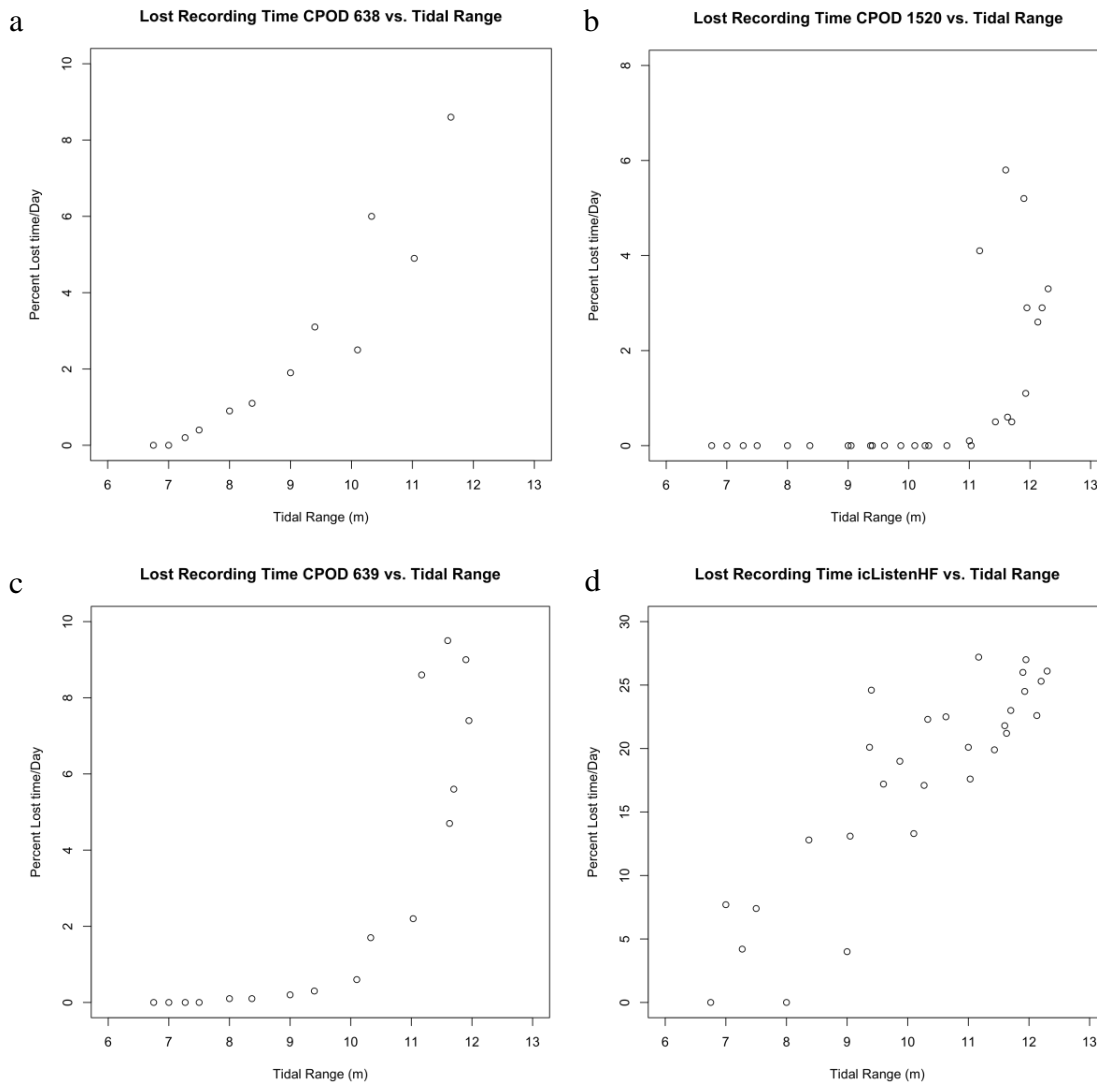


Figure 30. Percent lost recording time versus tidal range for a) C-POD 638, b) C-POD 1520, c) C-POD 639, and d) icListenHF. Y-axis scale varies among plots.

4.4.2 Hydrophone DPMs during Ebb and Flood Periods in Aug 2012

C-PODs 628 and 639, which were co-located with the icListenHF, showed a greater number of click train detections during ebb tide than flood tide, with peak detections on or near the 12th of August (neap tide) (Figure 31). Similar tidal cycle patterns in DPMs are shown for the icListenHF.

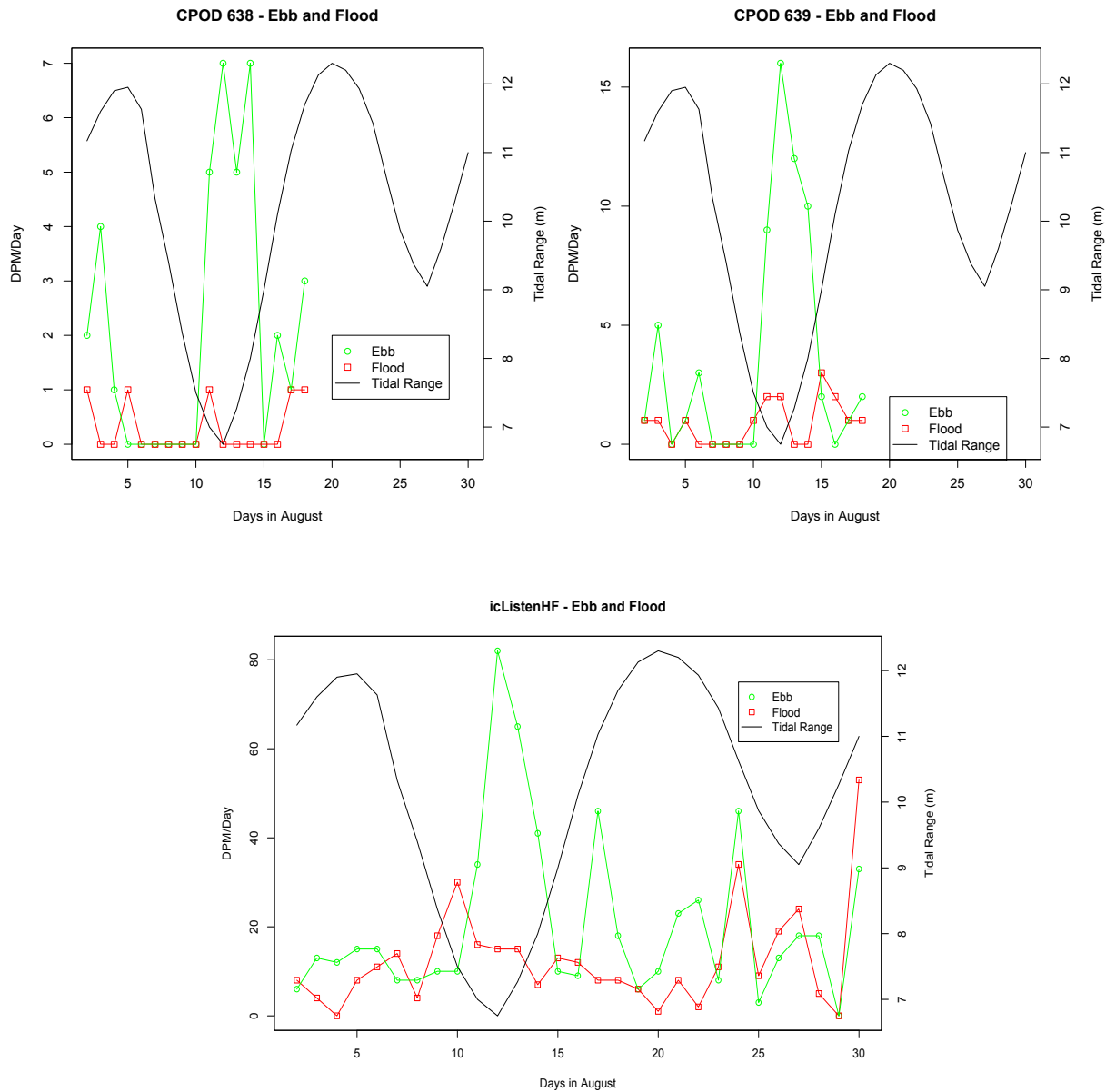


Figure 31. DPMs/day for both ebb and flood periods for C-POD 638, C-POD 639 and the icListenHF hydrophone during August 2012.

Figure 32 shows tidal height and porpoise click detections per minute over a single day for August 12th (neap tide) and August 22nd (spring tide). The majority of detections per minute on August 12th occurred on the ebb tide (after midnight) and at high slack water (mid-day). The majority of detections on August 22nd occurred on the ebb tide (before dawn) and during low slack water (at night). Interestingly, bursts of porpoise activity within the detection range were often followed by many hours of little or no detection.

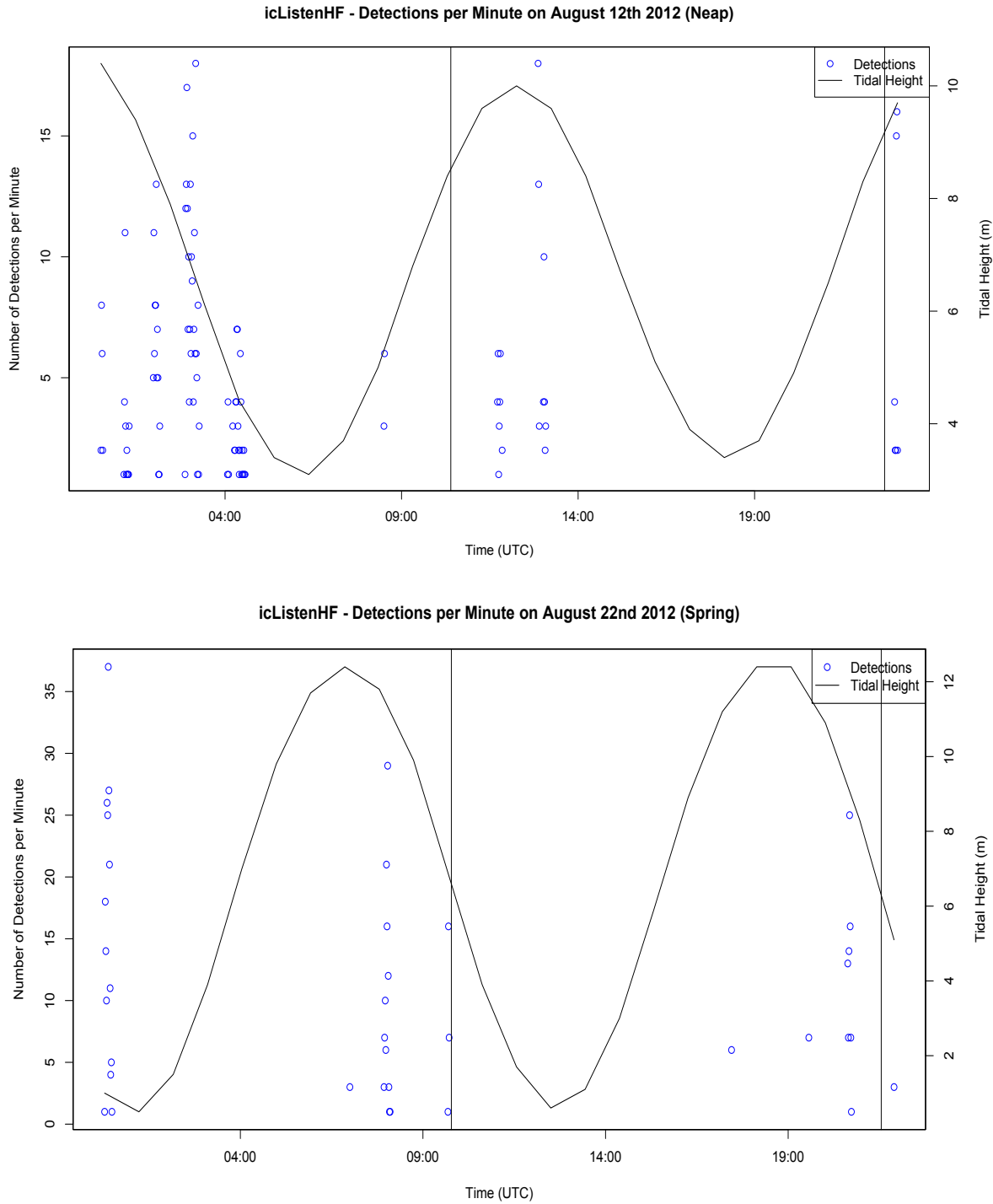


Figure 32. icListenHF detections per minute during August 12th (neap tide) and August 22nd (spring tide). Vertical bars represent sunrise and sunset respectively.

4.4.3 Comparison of Overall Detections

The icListenHF detected almost all of the click trains detected by the two co-located C-PODs (88% and 99%, Table 15). In many cases, the icListenHF recorded a DPM when one or both of the co-located C-PODs did not (Figure 33). This result most likely reflected the greater detection range and thus listening volume of the icListenHF hydrophone.

Table 15. Comparison of percent DPMs recorded by both C-PODs and the icListenHF hydrophone.

| | Distance from icListenHF (m) | C-POD DPMs also recorded by icListenHF (%) | icListenHF DPMs also recorded by C-PODs (%) |
|------------|---------------------------------|--|---|
| C-POD 638 | 48 | 88 | 6 |
| C-POD 639 | 67 | 99 | 13 |
| C-POD 1520 | 537 | 50 | 8 |

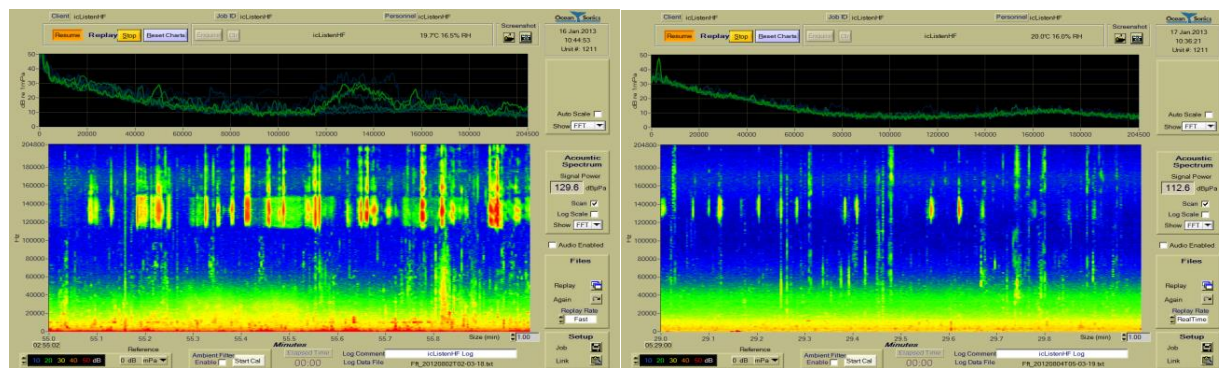


Figure 33. One minute LUCY screenshots with a high number of click detection events. Left, both the icListenHF and C-POD recorded a DPM. Right, the CPOD did not record a DPM during this minute which shows numerous faint clicks (i.e. clicks were beyond the detection range of C-PODs but within range of the icListenHF).

5.0 DISCUSSION

Porpoises are highly vocal animals, and wild individuals in Danish waters have been shown to produce sonar-click trains on average every 12.30 s (Akamatsu et al., 2007; Akamatsu et al., 1994). C-PODs log continuously 24 hours a day and are therefore useful for providing continuous data on porpoise activity within a few hundred meters (Brundiers et al., 2012). However it is important to stress, they only record porpoises that are actively echolocating and detection range is likely to vary depending on direction of travel and orientation of the porpoise. C-PODs (or their precursor, T-PODs) have still proved very useful in monitoring for impacts from offshore wind farms (Dähne et al., 2013; Tougaard et al., 2009), shipping noise (Polagye et al., 2011) and tidal turbines (Booth et al., 2011).

5.1 Porpoise Activity Trends in Minas Passage

This two year study highlights the use of C-PODs as a relatively cost-effective method to describe temporal and spatial patterns of porpoise activity in Minas Passage and thus provide a baseline for monitoring of tidal turbine testing at the FORCE site. Despite technical challenges, mainly related to the impacts of high flow velocity on the sensors, the study resulted in 1,932,410 minutes of recorded data from C-PODs at seven locations in Minas Passage over 397 days of monitoring. While porpoise were detected almost (98%) every day, they were only detected during 4.1% of the 10 minute detection periods in this study.

Our results suggest abundance of porpoise in Minas Passage is relatively low, and that they are using or moving through Minas Passage under certain environmental conditions. In comparison to other active or proposed tidal turbine sites, Minas Passage has moderate levels of porpoise detections. In Strangford Loch, Northern Ireland the DPM/day (reported from less sensitive T-PODs) was 4.5 during baseline studies before turbine installation (Booth et al., 2011). This contrasts with this study that found a mean of 40.6 DPM/day in Minas Passage, an order of magnitude higher. In Admiralty Inlet, Washington State, USA, Collar et al. (2012) reported median DPM/day of 152.9, approximately seven times the median DPM of 22/day found in this study in Minas Passage.

Julian Day and to a lesser degree Tidal Velocity, Tidal Height, % Time Lost, Day Night Index, and Location all had significant effects on the likelihood of porpoise click detection. Our GAM/GEE model result highlights porpoise are more likely to be detected in the spring and fall than during the summer and at moderately high tidal velocities and heights than low tidal velocities and heights. Porpoise detection rates were highest at the deepest locations and lowest in the most shallow monitoring location. Porpoise are most likely to be detected just after the middle of the night and least likely to be detected just after mid-day. As expected, an increase in % Time Lost, due to bedload transport noise and flow noise around the device/mooring unit during high flow velocities, reduces porpoise detections.

The fact that Julian Day is the largest driver of porpoise detection in Minas Passage is not surprising given the extreme changes in environmental conditions such as floating ice in the winter (Sanderson, Redden, and Broome, 2012) and prey availability (Crawford, 1979; Bradford & Iles, 1992) as well as the previously documented seasonal use of the Bay of Fundy by a number of marine mammal species, including harbour porpoise (Neave & Wright, 1968). Bearing in mind the sparsity of data from December to April, we document the highest seasonal detections during the spring (May) with detections decreasing until mid-summer (August) after

which detections increased into the fall (late October). Neave & Wright (1968) also found twin peaks in porpoise numbers in the southern Bay of Fundy, but with the first peak in July, two months later than what we document. They also found a mid-summer low in August and a fall peak in September, one month earlier than our fall peak. They suggest that females give birth in May/June shortly after returning to the Bay of Fundy and that their first peak in porpoise numbers coincides with the males and yearlings returning to the Bay of Fundy in July. They also suggest that the second peak in numbers in September coincides with the porpoise mating period. It may be that the porpoise in Minas Passage are following similar cycles, but that the timing of peak usage is spread out from May to October.

Three of the covariates in our model were directly or indirectly related to tidal cycles. Tidal velocity and height had higher explanatory power in our statistical model than % Time Lost did. There was a trend towards higher porpoise detections on flood tides between 0.5 to 2.5 m/s (average water column speed) and moderately high tides whereas detections decreased with increasing % Time Lost. Other studies have found increased porpoise presence during flood tides (Johnston et al., 2005; Sekiguchi, 1995). Johnston et al. (2005) provide compelling evidence that porpoise cover large areas, but concentrate in focal areas near islands, headlands and constricted channels, especially during flood tides. They found porpoise density in these areas during flood tides to be over five times porpoise density during ebb tides. This habitat use seems to be related to vortices in the water column and prey concentrations. These are likely to be the same drivers of porpoise presence in Minas Passage.

We found significant differences in porpoise detections across monitoring locations. The most parsimonious explanation for this is water depth. The majority of locations followed the trend of increasing porpoise detections with water depth. The only locations that deviated a little from this trend were E2 and S1. They were the two locations most affected by sediment noise (as shown by % Time Lost) which reduces porpoise detection. Gaskin et al. (1985) also found a positive relationship between depth (up to 100m) and porpoise presence. They attributed this to herring movement to deeper waters in the daytime. Another explanation is that as the depth of bottom-moored C-PODs increases, there is a corresponding increase in listening volume. This applies to both C-PODS and the lListenHF hydrophone, technologies which have maximum detection ranges up to 300 m and 1000 m, respectively. Likewise, an increase in tidal height (i.e. flood tide) increases the listening volume.

Diel variation in porpoise detections was also evident in this study. We found the highest porpoise detection rates in the early morning hours just after midnight, while the lowest detection rates just after noon. This pattern is consistent with other tidal turbine sites (Polagye et al., 2011; Booth et al., 2011) as well as other studies in the Bay of Fundy (Todd et al., 2009;

Haarr et al., 2009). It is possible that higher acoustic detections at night may be due to a switch from visual to acoustic foraging techniques.

The Click Max setting had a small but significant effect on porpoise detections. We increased the Click Max setting to overcome the memory saturation that occurs from sediment noise during tidal exchanges and thus decrease the % Time Lost. However, at the time of the change, the mooring riser length was increased by 1 m from the previous 2 m length in an effort to reduce damage to the SUB mooring units due to contact with the rocky bottom. The unexpected decrease in porpoise detections at the higher Click Max setting may be due to the units being farther off the bottom and thus exposed to faster currents which can create an increase in flow noise around the sensor and mooring unit.

The analyses conducted for this final report were more sophisticated than those presented in the interim reports. We included all of our data rather than just data with < 20 % Time Lost, and we modelled all covariates of interest at the same time, rather than running separate analyses. The benefit of modeling the variables at the same time is that it allows one to control for other variables. In spite of this, many of the trends we found in our interim reports still held in this final analysis. Seasonal trends shown in interim reports and this final report all found spring and fall peaks with a mid-summer low, however the GAM/GEE predicts those peaks two to four weeks earlier than the interim reports. This is likely due to earlier models excluding ~1/3 of the data with high % Time Lost. Diurnal and location trends were consistent across interim and final reports. Concurrent tidal data was not included for interim reports, except for June of 2011 at W1. Using tidal velocity at W1 in June 2011 and C-POD data with < 20% Time Lost we found an apparent peak in porpoise detections when the current was ebbing between 0.8 and 1.6 m/s. The descriptive statistics in this final report also found a similar trend with moderate (0 to -2 m/s) ebb tides having the highest porpoise detections. As mentioned, these descriptive statistics only consider a single covariate in isolation of all other covariates. The GAM/GEE model suggests that, especially for tidal velocity, it is necessary to control for other covariates at the same time. One plausible example of this is % Time Lost. Flood tides in Minas Passage generate larger periods of % Time Lost than ebb tides. As % Time Lost increases, porpoise detections decrease. If one doesn't control for this effect then it is likely that estimates of porpoise detections during flood tides will be under estimates.

5.2 Hydrophone Technology Comparisons

The comparison of different hydrophone technologies in a one month pilot study (August 2012) confirmed that noise generated by flows during spring tides was much greater than during neap tides. As a result, much of the detection time during spring tides was lost for both the icListenHF and C-POD hydrophones. Most of the high flow noise was likely due to moving

bedforms (Tollner et al., 2005) and the effects of tethered instrument moorings under strain (i.e. strumming, clanking of steel riser chains and shackles). This may explain why detections of harbour porpoise click trains were greater during the two neap tides (<9 m tidal range) in August than during the two spring tides (>11 m tidal range). During the entire month of August, peak harbour porpoise echolocation activity was recorded on August 12th when the tidal range was <7 m and % Time Lost was nil. Click train detections per minute, on what were considered high activity days (>600 detections per day), occurred primarily on ebb tides nearing low slack water at night. At these times of reduced current speed, porpoises may be following the movements of zooplanktivorous fishes, like herring, to surface waters.

Based on the manufacturer's claims of maximum detection range of the C-POD (300 m) and the icListenHF (1000 m), the potential listening volume of the icListenHF is up to 11x greater than for C-PODs. We have assumed that, under high flows, any flow-induced decrease in detection range (and hence listening volume) of the two-hydrophone technologies affects both technologies to the same degree. Although there are advantages to the larger listening volume of the icListenHF, the downside is that it detects and records more non-target noise (e.g. moving bedforms) than the C-PODs. This resulted in an icListenHF dataset with longer time periods over which harbour porpoise detections could not be identified, if present (i.e. lost recording time).

While the C-POD is a low cost autonomous hydrophone that can be deployed with a set of inexpensive D-cell batteries (internally housed) for up to 5 months at a time, it is not as physically durable as the icListenHF which showed no indication of malfunction when jolted in high flow, turbulent waters. However, the icListenHF is about twice as expensive per unit and requires the purchase of an external battery pack for deployments longer than a day. Currently, processing of the FFT files is not fully automatic (filters are under development), and thus requires considerable time in visually processing 1 min intervals (spectrum charts), unlike the C-POD software. Visual inspection of the raw data, however, reduces the chance of missing an event like a porpoise click train. In the Minas Passage, the icListenHF has a larger detection range (about 500 m, see Porskamp, 2013) than C-PODS (100-200 m) so fewer units would be required per area of coverage. Variability in the performance of icListenHF hydrophones remains unknown, as only one hydrophone was available for this study.

5.3 Conclusions and Recommendations

5.3.1 Temporal and Spatial Coverage

CPODs have been shown to be cost-effective in collecting long-term data in the challenging conditions of Minas Passage. This study successfully collected data late spring to late fall in multiple locations; however coverage was not complete across all locations. Coverage was best in the FORCE demonstration area. Continued monitoring at sites W1 and E1 (with FORCE lease area) is recommended. Two control sites outside of the demonstration area (W2 and S2) would allow BACI-type analyses. A regional scale deployment of 1-2 CPODs in Minas Basin and in the Minas Channel would permit a comparison with Minas Passage.

Very sparse data was collected over the winter and early spring period (December to April inclusive). Baseline data during winter prior to turbine installations at FORCE should be collected as soon as possible to allow for year-round comparisons (before and after turbine operation).

5.3.2 Deployment Methodology

The Minas Passage has proved a challenging location for deployment of CPODs. Despite one unit collecting data for a 167 day period, high tidal velocities resulted in a variety of malfunctions and memory capacity limitations leading to some data loss. Greater attention by the manufacturer to battery and SD card connections are required for continued use. Larger memory SD cards would partially solve memory saturation issues, but software upgrades to allow selection of an intermediate 'click max' setting would also be useful. The manufacturer has been informed of these recommendations. In locations where consistent data collection is imperative, duplication of CPODs is recommended. For short term fine-scale deployments (< 1 week), 'click max' settings at maximum may be appropriate, but unless larger memory SD cards are used, the standard 'click max' setting of 4096 is recommended for future monitoring studies.

This study highlighted the need to keep the SUB B3 streamlined instrument buoys at riser depths of 2m or below. An increase in riser heights to 3m appeared to increase the degree of memory saturation due to flow and sediment noise (Tollit et al., 2012). The use of tripods to deploy CPODs would increase the effort and cost overall but would reduce movement of the C-POD and would allow the deployment of concurrent monitoring devices (e.g., ADCP).

5.3.3 Alternative Monitoring Tools

This study included a pilot project to look at an alternative monitoring solution: a battery powered digital hydrophone and recorder, the iListenHF (Ocean Sonics Ltd). Deployment was limited to one month (due to power demands) and had higher start-up and post-processing cost. Like CPODs, successfully collecting data at very high tidal velocities was problematic and assessment of the use of different shielding methods to reduce flow noise around the sensor is recommended. Further concurrent deployments using a combination of C-PODs and digital

hydrophones are recommended for comparative purposes and greater coverage, especially during peak activity periods (spring and fall). Range testing of hydrophones under different flow scenarios would also help with interpretation of datasets collected. We recommend a cabled hydrophone be installed during TISEC deployments for long-term data collection near a tidal turbine.

While a fine-scale land-based observation study focussed on periods of high tidal velocity would be considered a useful validation of this study's results, observations at the extended range in turbulent conditions may not be reliable. New animal-borne tracking technology is becoming increasingly less invasive and more sophisticated. Porpoises have previously been captured in local weirs and tracked using satellite technology. A pilot study assessing the feasibility of such an approach is recommended to determine both regional habitat use by porpoises as well as fine-scale behaviour and vocal rates.

ACKNOWLEDGEMENTS

This project was funded by the Fundy Ocean Research Centre for Energy (FORCE) and the Offshore Energy Research Association (OERA) of Nova Scotia. We are grateful to Nick Tregenza and Chelonia Ltd. for their trouble shooting support of C-POD units and software, Ruth Joy and Monique MacKenzie for statistical advice. We thank Mark Wood and Chris Cook at Ocean Sonics Ltd for assistance with the use of the iListen hydrophone and Lucy software. The Ocean Tracking Network at Dalhousie University is thanked for providing acoustic releases. Field assistance was provided by Kaycee Morrison, Freya Keyser, Matthew Baker, Colin Buhariwalla, Duncan Bates and lobster boat captains Mark Taylor, Bob Vaughan and the late Croyden Wood Jr and their crews. Brian Sanderson is thanked for his contributions to providing tidal height and current speed data.

REFERENCES

- Akamatsu, T., Hatakeyama, Y., Kojima, T., & Soedo, H. (1994). Echolocation rates of two harbor porpoises (*Phocoena phocoena*). *Marine Mammal Science*, *10*(4), 401–411.
- Akamatsu, T., Teilmann, J., Miller, L. A., Tougaard, J., Dietz, R., Wang, D., Naito, Y. (2007). Comparison of echolocation behaviour between coastal and riverine porpoises. *Deep Sea Research Part II: Topical Studies in Oceanography*, *54*(3-4), 290–297. doi:10.1016/j.dsr2.2006.11.006
- Au, W., Kastelein, R., Rippe, T., & Schoonenman, N. M. (1999). Transmission beam pattern and echolocation signals of a harbor porpoise (*Phocoena phocoena*). *The Journal of the Acoustical Society of America*, *106*(6), 3699–3705.
- Bassett, C. (2010). *Underwater Ambient Noise at a Proposed Tidal Energy Site in Puget Sound*. University of Washington.
- Booth, C.G., Embling, C., Gordon, J., Calderan, S., & Hammond, P. (2013). Habitat preferences and distribution of the harbour porpoise *Phocoena phocoena* west of Scotland. *Marine Ecology Progress Series*, *478*, 273–285. doi:10.3354/meps10239
- Booth, C.G., Mackay, A., Northridge, S., & Sparling, C. (2011). *Acoustic Monitoring of Harbour Porpoise (Phocoena phocoena) in Strangford Lough. Report SMRUL-MCT-2011-16 to Marine Current Turbines*. (p. 52).
- Bradford R.G., Iles T.D. (1992). Unique biological characteristics of spring-spawning herring (*Clupea harengus* L.) in Minas Basin, Nova Scotia, a tidally dynamic environment. *Canadian Journal of Zoology*, *70*, 641-648.
- Brundiers, K., Clausen, K., Tougaard, J., Kyhn, L. A., Sveegaard, S., Thomas, L., Koblitz, J. C. (2012). Acoustic detection functions of C-PODs: estimating probability of detecting harbour porpoise clicks using playback experiments. In *European Cetacean Society* (p. 1). Galway.
- Cañadas, A., & Hammond, P. (2008). Abundance and habitat preferences of the short-beaked common dolphin *Delphinus delphis* in the southwestern Mediterranean: implications for conservation. *Endangered Species Research*, *4*, 309–331. doi:10.3354/esr00073
- Carlstrom, J. (2005). Diel variation in echolocation behavior of wild harbor porpoises. *Marine Mammal Science*, *21*(1), 1–12.
- Carstensen, J., Henriksen, O., & Teilmann, J. (2006). Impacts of offshore wind farm construction on harbour porpoises: acoustic monitoring of echolocation activity using porpoise detectors (T-PODs). *Marine Ecology Progress Series*, *321*, 295–308.

- Collar, C., Spahr, J., Polagye, B., Thomson, J., Bassett, C., Graber, J., Halvorsen, M. (2012). *Study of the Acoustic Effects of Hydrokinetic Tidal Turbines in Admiralty Inlet, Puget Sound* (p. 80).
- Cox, D. R., & Snell, E. J. (1989). *Analysis of Binary Data* (p. 240). Chapman and Hall CRC.
- Cox, T. M., Read, A. J., Solow, A., & Tregenza, N. (2001). Will harbour porpoises (*Phocoena phocoena*) habituate to pingers? *Journal of Cetacean Research and Management*, 3(1), 81–86.
- Crawford R. H. (1978). The biological survey of the Nova Scotia herring fishery. Nova Scotia Department of Fisheries, Manuscript and Technical Report Series, Project Report, 7905; p. 45
- Culik, B. M., Koschinski, S., Tregenza, N., & Ellis, G. M. (2001). Reactions of harbor porpoises *Phocoena phocoena* and herring *Clupea harengus* to acoustic alarms. *Marine Ecology Progress Series*, 211, 255–260.
- Dähne, M., Gilles, A., Lucke, K., Peschko, V., Adler, S., Krügel, K., Siebert, U. (2013). Effects of pile-driving on harbour porpoises (*Phocoena phocoena*) at the first offshore wind farm in Germany. *Environmental Research Letters*, 8(2), 025002. doi:10.1088/1748-9326/8/2/025002
- De Segura, A. G., Hammond, P. S., & Raga, J. A. (2008). Influence of environmental factors on small cetacean distribution in the Spanish Mediterranean. *Journal of the Marine Biological Association of the United Kingdom*, 88, 1185–1192.
- Ellis, J. I., & Schneider, D. C. (1997). Evaluation of a gradient sampling design for environmental impact assessment. *Environmental Monitoring and Assessment*, 48, 157–172.
- Embling, C. B., Gillibrand, P. a., Gordon, J., Shrimpton, J., Stevick, P. T., & Hammond, P. S. (2010). Using habitat models to identify suitable sites for marine protected areas for harbour porpoises (*Phocoena phocoena*). *Biological Conservation*, 143(2), 267–279. doi:10.1016/j.biocon.2009.09.005
- Envirosphere. (2009a). *Appendix 7 of the FORCE Environmental Assessment: Marine Seabirds and Marine Mammals* (p. 8).
- Envirosphere. (2009b). Oceanographic Survey, Oceanographic Measurements- Salinity, Temperature & Turbidity, Minas Passage Study Site. August 2008- March 2009.
- Envirosphere. (2010a). *Appendix H of the FORCE Environmental Assessment Addendum: Marine Mammal and Seabird Surveys Tidal Energy Demonstration Site — Minas Passage, 2009* (p. 58).

- Envirosphere. (2010b). Oceanographic Measurements- Salinity, Temperature, Suspended Sediment & Turbidity, Minas Passage Study Site, June-August 2009.
- Envirosphere. (2011a). *Appendix C of the Fundy Tidal Energy Demonstration Project Environmental Effects Monitoring Report: Marine Mammal and Seabird Surveys Tidal Energy Demonstration Site — Minas Passage , 2010* (p. 61).
- Envirosphere. (2011b). Oceanographic Measurements from Ships of Opportunity, Minas Passage Study Site, July 2010- January 2011.
- Fader, G. (2009). Geological Report for the Proposed In Stream Tidal Power Demonstration Project in Minas Passage, Bay of Fundy, Nova Scotia. Atlantic Marine Geological Consulting Ltd, Halifax, NS. 17 pp.
- Fader, G. (2011). Environmental Monitoring of Seabed Sediment Stability, Transport and Benthic Habitat at the Reference Site and the Vicinity of the NSPI TISEC Location in the Minas Passage. Atlantic Geological Consulting Ltd., Halifax, NS. pp 8.
- Fox, J., & Monette, G. (1992). Generalized Collinearity Diagnostics. *Journal of the American Statistical Association*, 87(417), 178–183.
- Fox, J., & Weisberg, S. (2011). *An R companion to Applied Regression* (Second Edi.). Thousand Oaks, CA: Sage.
- Gaskin, D. E., Read, A. J., Watts, P. F., & Smith, G. J. D. (1985). Population Dispersal, Size, and Interactions of Harbour Porpoises in the Bay of Fundy and Gulf of Maine. *Canadian Technical Report of Fisheries and Aquatic Sciences No. 1291* (p. 33).
- Genz, A., Bretz, F., Miwa, T., Mi, X., Leisch, F., Scheipl, F., & Hothron, T. (2012). *mvtnorm: Multivariate Normal and t Distributions. R package version 0.9-9994*.
- Haarr, M. L., Charlton, L. D., Terhune, J. M., & Trippel, E. A. (2009). Harbour Porpoise (*Phocoena phocoena*) Presence Patterns at an Aquaculture Cage Site in the Bay of Fundy, Canada. *Aquatic Mammals*, 35(2), 203–211. doi:10.1578/AM.35.2.2009.203
- Hardin, J. W., & Hilbe, J. M. (2002). *Generalized estimating equations* (2nd ed.). Chapman and Hall CRC.
- Hojsgaard, S., Halekoh, U., & Yan, J. (2006). The R Package geepack for Generalized Estimating Equations. *Journal of Statistical Software*, 15(2), 1–11.
- Johnston, D., Westgate, A., & Read, A. (2005). Effects of fine-scale oceanographic features on the distribution and movements of harbour porpoises *Phocoena phocoena* in the Bay of Fundy. *Marine Ecology Progress Series*, 295, 279–293. doi:10.3354/meps295279

- Karsten, R. H. (2011). An assessment of the potential of tidal power from Minas Passage, Bay of Fundy, using three-dimensional models. In *Proceedings of ASME 2011, 30th International Conference on Ocean, Offshore and Arctic Engineering*. Rotterdam, Netherlands.
- Karsten, R.H., McMillan, J.M., Lickley, M.J. & Haynes, R.D. (2008). Assessment of Tidal Current Energy in Minas Passage, Bay of Fundy. *Proceedings of the Institution of Mechanical Engineers, Part A: Journal of Power and Energy*, 222, 493-507.
- Karsten, R.H., Swan, A & Culina, J. (2013). Assessment of arrays of in-stream tidal turbines in the Bay of Fundy. *Phil. Trans. R. Soc. A*. 371: 20120189. Available at <http://dx.doi.org/10.1098/rsta.2012.0189>
- Koschinski, S, Culik, B., Damsgaard Henriksen, O., Tregenza, N., Ellis, G., Jansen, C., & Kathe, G. (2003). Behavioural reactions of free-ranging porpoises and seals to the noise of a simulated 2 MW windpower generator. *Marine Ecology Progress Series*, 265, 263–273. doi:10.3354/meps265263
- Koschinski, Sven, Dierderchs, A., & Amundin, M. (2008). Click train patterns of free-ranging harbour porpoises acquired using T-PODs may be useful as indicators of their behaviour. *Journal of Cetacean Research and Management*, 10(2), 147–155.
- Kyhn, L. A., Tougaard, J., Thomas, L., Duve, L. R., Stenback, J., Amundin, M., Teilmann, J. (2012). From echolocation clicks to animal density—Acoustic sampling of harbor porpoises with static dataloggers. *The Journal of the Acoustical Society of America*, 131(1), 550–560. doi:10.1121/1.3662070
- Liang, K.-Y., & Zeger, S. L. (1986). Longitudinal Data Analysis Using Generalized Linear Models. *Biometrika*, 73(1), 13–22.
- Lin, L. I. (1989). A concordance correlation coefficient to evaluate reproducibility. *Biometrics*, 45, 255–268.
- Macleod, K., Du Fresne, S., Mackey, B., Faustino, C., & Boyd, I. (2010). *Approaches to marine mammal monitoring at marine renewable energy developments. Final Report to the UK Crown Estate* (pp. 1–110).
- Marubini, F., Gimona, A., Evans, P., Wright, P., & Pierce, G. (2009). Habitat preferences and interannual variability in occurrence of the harbour porpoise *Phocoena phocoena* off northwest Scotland. *Marine Ecology Progress Series*, 381, 297–310. doi:10.3354/meps07893
- Money, J. H., & Trites, A. W. (1998). *A Preliminary Assessment of the Status of Marine Mammal Populations and Associated Research Needs for the West Coast of Canada: Final Report to Fisheries and Oceans Canada* (p. 62).

- Morrison, K. J. (2012). *Bottom substrate and associated epibenthic biota of the FORCE tidal energy site in Minas Passage, Bay of Fundy*. Honours thesis, Acadia University, Wolfville, NS..
- Neave, D. J., & Wright, B. S. (1968). Seasonal Migrations of the Harbor Porpoise (*Phocoena phocoena*) and Other Cetacea in the Bay of Fundy. *Journal of Mammalogy*, *49*(2), 259–264.
- Ocean Sonics Ltd. (2012). *icListen operations guide*. Great Village, Nova Scotia, Canada.
- Oceans Ltd. (2009). *Appendix 5 of the FORCE Environmental Assessment: Currents in Minas Basin* (p. 170).
- OEER. (2008). *Fundy Tidal Energy Strategic Environmental Assessment Final Report* (p. 92).
- Olesiuk, P. F., Nichol, L. M., Sowden, M. J., & Ford, J. K. B. (2002). Effect of the Sound Generated By an Acoustic Harassment Device on the Relative Abundance and Distribution of Harbor Porpoises (*Phocoena phocoena*) in Retreat Passage, British Columbia. *Marine Mammal Science*, *18*(4), 843–862.
- Palka, D. (1996). Effects of Beaufort Sea State on the Sightability of Harbor Porpoises in the Gulf of Maine. *Report of the International Whaling Commission*, *46*, 575–582.
- Panigada, S., Zanardelli, M., MacKenzie, M., Donovan, C., Mélin, F., & Hammond, P. S. (2008). Modelling habitat preferences for fin whales and striped dolphins in the Pelagos Sanctuary (Western Mediterranean Sea) with physiographic and remote sensing variables. *Remote Sensing of Environment*, *112*(8), 3400–3412. doi:10.1016/j.rse.2007.11.017
- Philpott, E., Englund, a., Ingram, S., & Rogan, E. (2007). Using T-PODs to investigate the echolocation of coastal bottlenose dolphins. *Journal of the Marine Biological Association of the UK*, *87*(01), 11. doi:10.1017/S002531540705494X
- Pierpoint, C. (2008). Harbour porpoise (*Phocoena phocoena*) foraging strategy at a high energy, near-shore site in south-west Wales, UK. *Journal of the Marine Biological Association of the United Kingdom*, *88*(06), 1167–1173. doi:10.1017/S0025315408000507
- Polagye, B., Wood, J. D., Bassett, C., Tollit, D., & Thomson, J. (2011). Behavioral responses of harbor porpoise to vessel noise in a tidal strait. *Journal of the Acoustical Society of America*, *129*(4), 2368.
- Porskamp, P. (2013). *Passive acoustic detection of harbour porpoises (Phocoena phocoena) in the Minas Passage, Nova Scotia, Canada*. Honours thesis, Acadia University, Wolfville, NS.
- R Core Team. (2012). *R: A language and environment for statistical computing*. Vienna, Austria.

- Ryan, P. C. (2010). *OEER / FORCE Tidal Energy Workshop Report* (p. 24).
- Sanderson, B. G., Redden, A. M., & Broome, J. E. (2012). *Sediment – Laden Ice Measurements and Observations, and Implications for Potential Interactions of Ice and Large Woody Debris with Tidal Turbines in Minas Passage. Final Report submitted to the OEER/OETR* (p. 64).
- Sekiguchi, K. (1995). Occurrence, behavior and feeding habits of harbor porpoises (*Phocoena phocoena*) at Pajaro Dunes, Monterey Bay, California. *Aquatic Mammals*, 21(2), 91–103.
- Shaw, J., Todd, B.J., Li, M.Z., and Wu, Y. (2012). Anatomy of the tidal scour system at Minas Passage, Bay of Fundy, Canada. *Marine Geology*, 323, 123-134.
- Skov, H., & Thomsen, F. (2008). Resolving fine-scale spatio-temporal dynamics in the harbour porpoise *phocoena phocoena*. *Marine Ecology Progress Series*, 373, 173–186.
- Stewart, P.L. (2009). Hard Bottom Sublittoral Benthic Communities in Areas Proposed for In-Stream Tidal Power Development, Northern Minas Passage, Bay of Fundy. Pages 44-57, in Redden, A.M., J.A. Percy, P.G. Wells and S.J Rolston (Eds.) Resource Development and its Implications in the Bay of Fundy and Gulf of Maine. Proceedings of the 8th Bay of Fundy Science Workshop, Wolfville, Nova Scotia, 26-29 May 2009. Bay of Fundy Ecosystem Partnership Technical Report No. 4, Wolfville, NS. 382 pp.
- Todd, V. L. G., Pearse, W. D., Tregenza, N. C., Lepper, P. A., & Todd, I. B. (2009). Diel echolocation activity of harbour porpoises (*Phocoena phocoena*) around North Sea offshore gas installations. *ICES Journal of Marine Science: Journal du Conseil*, 66(4), 734.
- Tollit, D., Wood, J., Broome, J., & Redden, A. (2011). *Detection of Marine Mammals and Effects Monitoring at the NSPI (OpenHydro) turbine site in the Minas Passage* (p. 36).
- Tollit, D., Wood, J., Redden, A., Fogarty, L., & Broome, J. (2012). *Passive Acoustic Monitoring of Cetacean Activity Patterns and Movements Relative to Pre and Post deployment of TISEC devices in Minas Passage: Year 1 Interim Report* (p. 49).
- Tollner, E.W., Rasmussen, T.C., Upchurch, B., and Sikes, J. (2005.) Simulated moving bed form effects on real-time in-stream sediment concentration measurement with densitometry. *Journal of Hydraulic Engineering* 131(12), 1141-1144.
- Tougaard, J., Carstensen, J., Teilmann, J., Skov, H., & Rasmussen, P. (2009). Pile driving zone of responsiveness extends beyond 20 km for harbor porpoises (*Phocoena phocoena* (L.)). *The Journal of the Acoustical Society of America*, 126(1), 11–14. doi:10.1121/1.3132523
- Venables, W. N., & Ripley, B. D. (2002). *Modern Applied Statistics with S*. (Fourth Edi.). New York: Springer.

- Verfuss, U. K., Honneff, C. G., Meding, A., Dahne, M., Mundry, R., & Benke, H. (2007). Geographical and seasonal variation in harbour porpoise (*Phocoena phocoena*) presence in the German Baltic Sea revealed by passive acoustic monitoring. *Journal of the Marine Biological Association of the United Kingdom*, *87*(1), 165–176.
- Walker, C. G., MacKenzie, M. L., Donovan, C. R., & O’Sullivan, M. J. (2011). SALSA -a spatially adaptive local smoothing algorithm. *Journal of Statistical Computation and Simulation*, *81*(2), 179–191.
- Wilson, B., Batty, R. S., Daunt, F., & Carter, C. (2007). *Collision risks between marine renewable energy devices and mammals, fish and diving birds. Report to the Scottish Executive* (pp. 1–110). Oban, Scotland.
- Wood, S. N. (2011). Fast stable restricted maximum likelihood and marginal likelihood estimation of semiparametric generalized linear models. *Journal of the Royal Statistical Society (B)*, *73*(1), 3–36.
- Wu, Y., Chaffey, J., Greenberg, D. A., Colbo, K., & Smith, P. C. (2011). Tidally-induced sediment transport patterns in the upper Bay of Fundy: A numerical study. *Continental Shelf Research*, *31*(19-20), 2041–2053. doi:10.1016/j.csr.2011.10.009